A THESIS REPORT

On

Bond Graph Modelling and Simulation of Walking Mechanism of Quadruple Robot

Submitted in partial fulfilment of the requirement

for the award of degree of

Master of Engineering
in
CAD/CAM Engineering

Submitted by

Garima Soharu

Roll No.: 801584005

Under the guidance of

Dr. Tarun Kumar Bera

Associate Professor

Department of Mechanical Engineering

Thapar University, Patiala

DEPARTMENT OF MECHANICAL ENGINEERING

THAPAR UNIVERSITY

PATIALA-147004, INDIA

July-2017

Declaration

I hereby declare that work done in this thesis report entitled, "**Bond Graph Modelling and Simulation of Walking Mechanism of Quadruple Robot**" submitted towards partial fulfilment of requirement for award of **Master of Engineering degree** in **CAD/CAM Engineering** in **Mechanical Engineering Department** of **Thapar University, Patiala**, is an authentic record of work carried out by me under the supervision and guidance of **Dr. Tarun Kumar Bera, Associate Professor** of **Mechanical Engineering Department, Thapar University, Patiala**.

This matter embodied in this report has not been submitted in part or full to any other university or institute for the award of any degree.

DATE: 17-7-2017

Garima

Garima Soharu

This is to certify that above declaration made by the student concerned is correct to the best of my knowledge and belief.

17/7/17

Dr. Tarun Kumar Bera

Associate Professor

Mechanical Engineering Department

Thapar University, Patiala

Acknowledgement

"Look at a stone cutter hammering away at his rock, perhaps a hundred times without as much as a crack showing in it. Yet at the hundred-and-first blow it will split in two, and I know it was not the last blow that did it, but all that had gone before".

-Jacob A. Riis

Journalist, Photographer

The above proverb completely summarizes the effort that has gone in completing this thesis and the M.E course. Nevertheless, a special mention is required that the stonecutter was not alone in this journey. There were lot of people who kept the stonecutter's morale and spirit high so that she can keep on hammering and not give up after few blows of failure.

A teacher is given place above God so I would start with thanking my guide **Dr. Tarun Kumar Bera,** Associate Professor, Mechanical Engineering Department, Thapar University, who introduced me to the field of research, especially to the new area of bond graph modelling. He has unconditionally supported me not only in my thesis but academically and emotionally. He was always there to encourage me whenever I felt demotivated. He has not provided me with only academic lessons but the lessons for life that includes high work ethics and complete sincerity towards work taken in hand. He is the most hardworking person I have ever met and an inspiration for me. It would be an honour for me if I could become half as good teacher as him.

The environment you work in has lot of effect on your performance; it is made by your seniors and peers. I have been lucky to get the best of the lot in terms of both seniors and peers. I would like to thank **Mr. Navjot Gill** who was there with me in my first year of M.E and guided me throughout my course to work hard. He was the one who guided me to choose Dr. Bera as my guide and I can't thank him enough for this. I met **Mr. Vikram Singh Jamwal** during my thesis work; it would be no exaggeration if I say it was because of him that I was able to complete my thesis writing on time. He is also responsible for keeping my sanity during thesis work. However, he is younger to me in age but he has become the elder brother I never had. I would now thank my family away from home here **Jasmine, Sharanjit, Sukhmani, Shairy, Tanvi, Joypreet and Amardeep** who made my stay in Thapar University full of fun and good memories.

I finish with my family. No words can express how lucky I am to have such an amazing family, unique in many ways, and the stereotype of a perfect family in many others. Their support has been unconditional all these years; they have given up many things for me to be a postgraduate. Thank you to my parents **Mr. Devinder Singh Soharu** and **Ms. Raksha Soharu** for giving me best of everything throughout my life. It was because of you both taking care of my son I was able to give my 100% to my work. **Maj. Hemanshu Singh Bhandari** thank you for being my stress buster, for listening everything about my research without knowing anything about my work. Your unconditional support has made my belief in institution of marriage stronger. Last but definitely not the least I would like to thank my son **Rudra Pratap Singh Bhandari** for being such a patient and brave kid for staying away from his mother for two long years for letting her achieve her dreams. Also my apologies for missing your birthdays, first day to school and many more occasions where you needed me.

Garima Soharu

Abstract

Legged robots have capability of traversing any type of terrain with much ease and stability compared to wheeled robots. The uniqueness of legged robots are that they don't have continuous contact with ground thus helping them select their footsteps to avoid obstacles. Other advantageous properties of legged robots are that they cause less damage to the terrain, their ability to bend on the joints give the property of active suspension, and they can walk in every direction, which gives them leverage to navigate through crowded and compact surroundings. The objective of this thesis is to model and simulate a walking mechanism for quadruple model which is stable and is able to implement different types of gaits. The stability control of legged robot is of utmost importance as compared to wheeled robot as contact from ground is discontinuous due to lifting and placing of leg. The positing of legs relative to body of robot considerably effects the stability, also the sequence and timing in which legs are moved and placed play important role in energy efficiency. Here three models for walking mechanism has been developed using bond graph technique. First the mechanism for two legs is modelled, further two different models for walking of quadruple have been developed. Results from simulation are discussed. The comparison of different gaits are done for energy efficiency.

Key words: Locomotion; Gaits; Bond graph modelling; Planar model; Quadruple; Stability.

Nomenclature

C_m	Capacitance of motor
I_m	Moment of inertia of motor
I_b	Moment of inertia of body
I_w	Moment of inertia of leg
K_l	Compliance element of leg's
$K_{m_{f1}}$	Compliance element of front leg's Link
$K_{m_{f2}}$	Compliance element of front leg's Link2
$K_{m_{r1}}$	Compliance element of rear leg's Link1
$K_{m_{r2}}$	Compliance element of rear leg's Link2
L_{leg}	Length of complete leg
l_1, l_2	Distance of front and rear wheel from COG
M_b	Mass of body
R_m	Resistance of motor
U	Velocity in x direction
V	Velocity in y direction
β	Angular rotation in y direction
λ	Differentiability constant
μ_1	Modulus of Gyrator for motor of front Leg's Link1
μ_2	Modulus of Gyrator for motor of front Leg's Link2
μ_3	Modulus of Gyrator for motor of rear Leg's Link1
μ_4	Modulus of Gyrator for motor of rear Leg's Link2

Subscripts

B	Body
f1	Front leg Link1
f2	Front leg Link2
M	Motor
r1	rear leg Link1
r2	rear leg Link2
U	Linear velocity in *x* direction
V	Linear velocity in *y* direction
W	Link
ω	Angular rotation in z direction

List of Figures

List of Tables

Table of Contents

Chapter 1

Introduction

Walking robots have become quite popular because of their ability to walk in terrains that are inaccessible to humans and wheeled robots. Their ability to walk like animals makes it easy for them to walk on difficult terrains. While designing the walking robot we need to develop a model that provides the desired locomotion to the robot. This thesis focuses on developing various gaits to achieve the desired locomotion. The benefit of these robots are that they don't roll on surface instead they use footsteps to move, which helps them to overcome obstacles easily, as compared to the wheeled robots who have to traverse according to terrain. Further legs can bend like knees at their joints helping the body of robot to move up and down. In addition, these robots can move in every direction i.e. they can move ahead, left right and can turn.

The above-mentioned benefits of walking robot can be achieved by how we design its mechanical system and controls. The designing of the legged robot is very complex. A legged robot has large degrees-of-freedom that increase its complexity, also adding on to the weight and price. A large number of degrees of freedom make its control to deal with non-linear systems. In addition, it has to deal with its varying dynamics where the leg is moving up and down, its foot's contact with ground further add on to unknown dynamics. Stability is also a major concern, as we have to figure out how to support the system when the legs are in a flight phase and when they are placed back on the ground.

This thesis emphasizes on the application of the bond graph approach in the modelling and simulation (using Symbol Shakti software) of quadruple robot using the methodology which nature has provided us. By nature, we mean the gait of animals that has evolved through millions of years. They have optimum stability measure while lifting their legs and moving forward, they switch their gaits according to the requirement of speed and terrain. Though it is not possible to completely replicate their motion as, it includes various neurological and muscular parameters. However, we have tried to replicate the various gaits of horses in our work.

Bicycle model has been taken as the basis for modelling the robot where the wheels are replaced by legs and the vehicle body by the robots body. The legs are made up of two rigid links. The lower link has contact with the ground that gives it the resistance while moving thus making the body move forward. The vehicle body is a rectangular frame with the all four legs attached to its corners. Each link has a motor attached to it that gives it the power to achieve the desired locomotion.

First, we modelled the bicycle model using bond graph approach with two legs, the front and the rear legs. The model is then simulated for checking the stability of the model. Implementation of the various gaits is not possible with the two legs thus we further converted the same model into four leg model in bond graph and varied the supply of motor to the legs to achieve various gaits. The gaits are of two types dynamically stable and statically stable. Dynamically stable gaits have more speed as compared to statically stable gaits, in them two legs are in flight phase and the other two legs are at ground for support. On the other hand the statically stable gaits are slow in speed, we can also say it's a walking gait or a crawl gait, in which, at a time only one leg is lifted and the other three legs remain at ground for support. This type of gait is used when the robot has to take a turn.

1.1 Background and Motivation

Mobile robots have found applications in various fields like entertainment, defense, hospitality and housekeeping. Lots of research and development have been done in this field specially related to the wheeled robots. They have been extensively being used in areas where human interaction is risky. The other type of mobile robots are walking robots or legged robots that unlike wheeled robots have footstep movement rather than rolling motion. Wheeled robots have a constraint that they cannot access every terrain because its movement is dependent on the contour of terrain. Whereas the legged robots movement is independent of the contour of terrain, it has additional advantage that it can choose its gait according to the movement required while traversing the terrain. Legged robot's ability to tilt up and down likes legs bend at knee joint give additional advantage to adjust itself in any type of terrain. The motivation for designing a quadruple robot model is to be able to replicate the motion given to us by nature in the form of locomotion of the animals. Thus to study and model, the various gaits of animals are analyzed the dynamics of the body and legs. We have modelled the leg and body in bond graph and combined them in the main bond graph model to achieve the desired gaits. We have taken a different approach of modelling it by taking bicycle model as the basis. Two motors have been attached to each link of leg and then their movement is controlled by varying the power supply to the motors. In addition, the gaits have been developed by switching the motor supply to the legs in the desired pattern of the gaits.

The Quadruple model is a four-legged model taking planar model as the basis of modelling. It has been tried to achieve the gaits used by the animals. However, it is difficult to model the animal's gait completely because it has lot of neural and muscular control. But yes there are many manoeuvres which can be done by a robot but not the actual animal. It has been seen in the previous section that the legs are completely following the motion desired.

1.2 Types of Gaits

The locomotion of the robot has been derived using various gaits. As discussed before the gaits are of two types dynamically stable and statistically stable. The dynamically stable gaits are trot gate, pace gait and bound gait. Whereas statically stable gaits are amble gait, in which one leg moves at a time and the other three legs remain on ground for stability.

1.2.1 Statically Balanced Gaits

The statically balanced gait is also known as amble gait. In amble gait only one leg moves forward and rest of the legs remain on ground. The speed of this gait is slow. But this is the most stable gait as the center of gravity of the body always remains inside the triangle formed by the legs which are on ground. The order of movement of legs can be any according to the requirement of terrain and situation. Amble gait following order 1-4-2-3 is shown in Fig. 1.1.

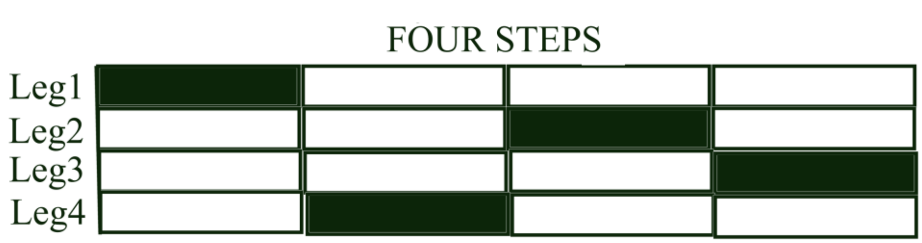

Fig. 1.1 Amble gait

1.2.2 Dynamically Balanced Gaits

The dynamically balanced gaits are those in which the legs move in pair. They are further classified into various types of gaits explained below:

- Trot Gait

In trot gait, the diagonally opposite legs move together whereas the other diagonally opposite legs remain on ground. The trot gait is generally used by horses while racing because it is to bring variation in speed using this gait.

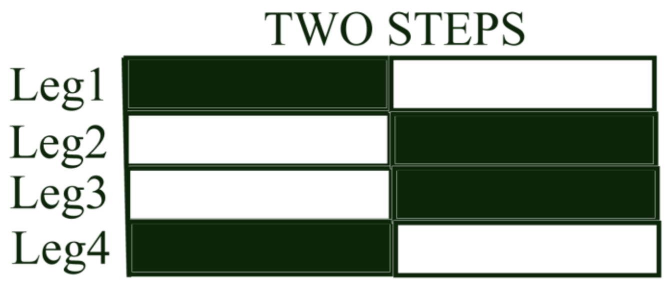

Fig. 1.2 Trot gait

- Pace Gait

In pace gait the front and rear right leg move together and front and rear left leg move forward together. The animal generally uses this type of gait when it has to balance its weight while moving forward. This gait is generally used by wide-bodied animals.

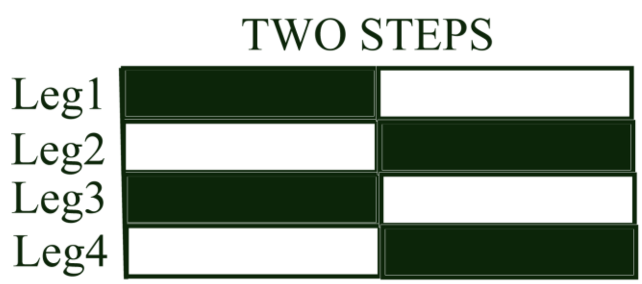

Fig. 1.3 Pace gait

- Bound Gait

In bound gait both the front legs move together and rear legs move together. This gait is also called gallop gait. Rabbits and rodents generally use this gait.

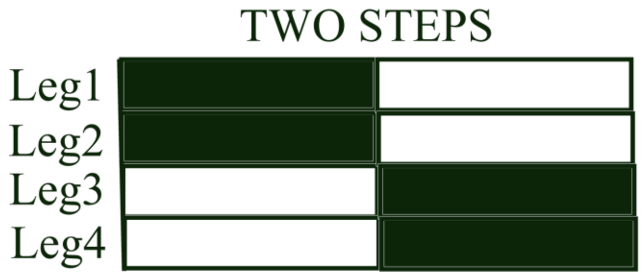

Fig. 1.4 Bound gait

1.3 Bond Graph Approach

Bond graph modelling technique is a technique that is algorithmic and uniform in nature. Bond graph works on the principal that every system has energy interactions among them that flow in and out of the elements that comprise the system. It is bidirectional i.e. it tells us what is going inside and coming outside from a system through casualty. The beauty of this technique is that it can model a system in any energy domain and it derives the differential equations itself. Thus, it is the best option for modelling the Quadruple robot, as it is a non-linear system.

1.3.1 Introduction to Bond Graph

The bond graph comprises of seven elements I, R, C, SF, SE, GY and TF that are connected to junctions 1, 0 by a line segment called bond. The direction of bond represents the flow of power. Casualty is the cause and effect relationship among elements and junctions. It is represented by the casual stroke. If the casual stroke is towards the junction then the element is giving effort to the junction and taking flow from the system. On the other hand if the casual stroke is towards the element then it is getting effort from the system and giving flow to the system. Thus, we can say that the power transmission in bond graph is the product of its cause and effect.

$$P = E * f \tag{1.1}$$

Where $P = Power, E = Effort, f = flow$

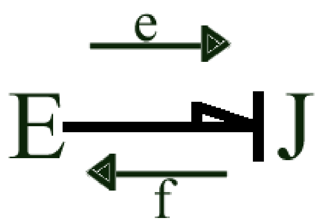

Fig. 1.5 Junction and element with casual stroke

Classification of a bond graph junction can be done as follows:

- **Junctions**

1-Junction–It is also called the series junction deriving its inference from electrical series circuit which has equal flow. Similarly 1–junction is equal flow junction and it can also be called flow sum junction. Thus the elements connected to 1–junction will have same flow.

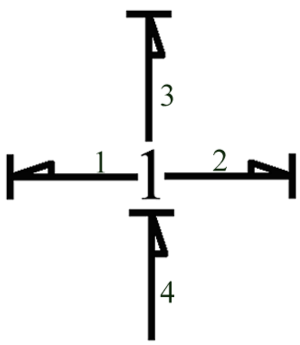

Fig. 1.6 Representation of 1-junction

$$e_1 f_1 + e_2 f_2 + e_3 f_3 + e_4 f_4 = 0 \tag{1.2}$$

Since,

$$f_1 = f_2 = f_3 = f_4 \tag{1.3}$$

Thus,

$$e_1 + e_2 + e_3 + e_4 = 0 \tag{1.4}$$

0-Junction– It is also called parallel junction. Just like 1-junction it also takes its inference from electrical parallel circuit which has equal effort and is flow some junction. Thus, the elements connected to this junction has equal effort.

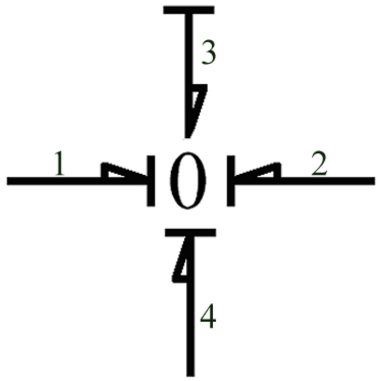

Fig. 1.7 Representation of 0-junction

$$e_1 f_1 + e_2 f_2 + e_3 f_3 + e_4 f_4 = 0 \tag{1.5}$$

Since,

$$e_1 = e_2 = e_3 = e_4 \tag{1.6}$$

Thus,

$$f_1 + f_2 + f_3 + f_4 = 0 \tag{1.7}$$

- **Elements**

As mentioned earlier that bond graph has seven elements. These elements can be further divided into single port elements (I, C, R), two port elements (GY, TF) and sources (SE, SF).

Compliance element:

It is represented by letter ‘C’. It is the element which stores the energy of system like spring does in mechanical system. The bond connecting it with junction has causal stroke towards the junction always, thus making it integral element. It is pictorially represented in Fig. 1.2.

Fig. 1.8 Representation of compliance element

Inertial element:

It is represented by letter ‘I’. This element is the representation of the mass points in system. The bond connecting this element with the junction has its casual stroke towards element. It also has integral casualty. It is pictorially represented in Fig. 1.3.

Fig. 1.9 Representation of inerta element

Resistive element:

It is represented by letter ‘R’ it is an energy dissipating element like a damper in mechanical system. Its casual stroke can be on any side. Thus it can be both differentially and integrally causable. It is pictorially represented as shown in Fig. 1.4.

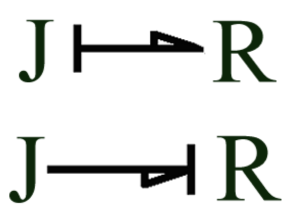

Fig. 1.10 Representation of resistance element

Source of effort:

Source of effort is represented by letters ‘SE’. This element governs the energy flow in the system. It only gives energy to the system and does not take anything in return. Pictorially, it may be represented as shown in Fig. 1.5.

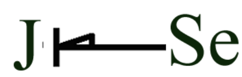

Fig. 1.11 Representation of source of effort element

Source of flow:

Source of flow is represented by letter ‘SF’. This element governs the flow in system. It only gives flow to system and does not take anything in return. Pictorially, it may be represented as shown in Fig. 1.6.

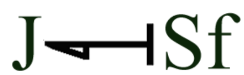

Fig. 1.12 Representation of source of flow element.

Transformer:

The transformer converts flow into flow by multiplying it with a modulus, same goes for the effort. It is used where the flow or effort from one junction is to be magnified or reduced while transferring it to other junction. It further plays an important role in coordinate transformations. It is as shown in Fig. 1.7.

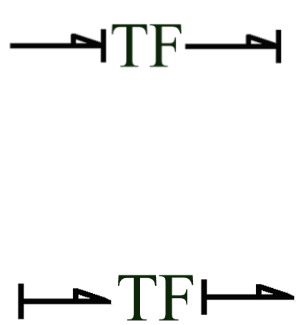

Fig. 1.13 Representation of transformer element

$$f_1\mu = f_2 \tag{1.8}$$

$$e_2\mu = e_1 \tag{1.9}$$

Gyrator:

The Gyrator is an element which is used when effort from one junction is to be converted to flow for another junction. It derives its inference from the gyroscopic effect. A gyrator element is as shown in Fig. 1.8.

Fig. 1.14 Representation of gyrator element

$$f_1\mu = e_2 \tag{1.10}$$

$$f_2\mu = e_1 \tag{1.11}$$

1.6 Contribution of Thesis

- Bond graph model of two legged planar model
- Simulations of angular movements of link and there linear displacements
- Mathematical formulation and programming for desired motion
- Bond graph model of quadruple robot based on planar model
- Simulation results for different gaits and comparison of displacements achieved in all the gaits
- Bond graph model for alternative three dimensional model
- Simulations results for pace gait implemented in the model

1.7 Organization of Thesis

This thesis work is divided into 5 chapters that can be summarized as follows:

Chapter 1 introduces the bond graph technique for modelling systems in detail. In addition to this, it also introduces the locomotion of legged robot and various gaits followed by it.

Chapter 2 presents literature review done in order to complete this thesis. It very clearly explains about the literatures surveyed in different fields like robot locomotion, control and implementation of various gaits and bond graph.

Chapter 3 is dedicated to modelling of two-legged planar model. This chapter contains bond graph model of links, legs and planar model. Simulation results are also discussed in this chapter itself.

Chapter 4 deals with modelling of both the quadruple model and three-dimensional model .It contain the detail the kinematic relations and bond graph for both the models. Simulation results are also discussed in chapter itself.

Chapter 5 presents conclusions obtained from the research work conducted during thesis work. In addition to this, this chapter also deals with future scopes of the thesis.

Chapter 2

Literature Review

2.1 Introduction

This chapter dissertates the literature review done for consummation of the thesis and the objectives of the thesis. Literature review was carried on in three areas: (i) Dynamics of robot body and legs, (ii) Various gaits and their implementation and (iii) Bond graph modelling technique.

2.1.1 Literature Review on Dynamics of Robot Body and its Legs

The use of behavior of body dynamics in control of locomotion of robot presents lot of challenges, as it can increase the intricacy of design and effect the speed. Behavior variations in body dynamics are analyzed by varying the values of control parameters. Thus it is found that a single parameter can control the forward velocity and different types of gaits. Using the elastic leg bound gait was achieved without using the feedback sensors. The body dynamics which are required to be handled (i) regulating the height leg when step is taken (ii) maintaining the orientations of body (iii) control of the speed for going forward .The walking of robot is divided into two phases, i.e., stance phase and flight phase. The stance phase is when feet is lifted from ground to start walking and flight phase when is feet is in air moving forward. For stance phase the dynamics (i) and (ii) are to be maintained and (iii) for flight phase [**1**].

Further, the behavior of body dynamics can be divided into three essential activities: to support the body through hopping in vertical direction, controlling the position of body by following the motion developed by hip torques during each step taken by leg and to keep body stable following basic symmetry principle. Thus an algorithm is developed to control the behavior of body dynamics through interaction between kinematics of body and the reaction force applied on robot feet by ground. The robot used for experimentation is Big Dog. Systems that provide power, controls and sensing are onboard on this robot. It has two- stroke internal combustion that is water-cooled for power supply. The two-stage servo valves regulate the actuators which are hydraulic cylinders. There are sensors at each actuator for sensing force, joints position, and operational support. There are fifty sensors in BigDog. Attitude and acceleration are measured by inertial sensors, while motion and force at the working joints of actuators are measured by joint sensors.

These sensors give information to the computer onboard about the position of the robot in space [**2**].

The robot can be powered by electric system and hydraulic system that is powered by an engine. The advantage of hydraulic system is: it compresses the size of robot and increases it load carrying capacity, greater strength, refueling is faster process then recharging, quick dynamic response making robot more stable, it is more conducive to supply energy to joints as per real time needs [**3**].

The electrically powered actuators are preferred due to their simplicity, low cost, higher accuracy and compact size. Both the systems can be used together; hydraulic system is used for forward/backward motion and electrical system for lateral motion. The compliance element does not only permit the system to adapt to irregularities in terrain but also reduce consumption of energy and obtain power peaks mechanically, which are not possible in stiff structure. But its dynamic is more complex than stiff robot. The oscillations of high amplitude are induced and the low natural frequency is produced due to intrinsic compliance. This problem can be encountered by lowering the bandwidth considerably as compared to rigid body. But this lowers the performance of the robot. It can be overcome if stiffness and damping coefficient are selected according to ground, mass and kinematics properties. The devices with variable stiffness can be useful, but they are currently difficult to apply [**4**].

A compliant four-legged robot has been developed for fast, efficient and versatile locomotion. It is driven by highly compliant system joined in series elastic actuation that makes control of torques easier, it has good impact bearing capacity thus making it suitable for highly dynamic movements. Taking inspiration from natural locomotion the research in field of locomotion of legged robot is going substantial changes. Nowadays more compliant system are offering new aspect to research field as compared to old stiff and kinematically controlled systems. They are perfect to interact with their surroundings because of mechanical flexibility due to low system inertia. They can easily avoid jerks from ground and can easily work with human operators. They are equivalent to muscle and tendons in nature in behavior [**5**].

2.1.2 Literature Review on Various Gaits and their Implementation

Application in rough and highly unstructured terrain must be the goal of legged robots. The current infrastructure is capable of providing locomotion in these types of terrain. One thing that could be done is that pre feed the properties or terrain maps in the robot. However, this is not possible in real life cases, thus an additional feature called perception needs to be added to the system. Based on the above needs, a robot named the ALoF was introduced to study perception. A crawling gait was implemented for locomotion on surfaces with loose soil. The purpose of this robot is not only application of feature of perception but also the stability in highly difficult terrains [**6**].

Application of robots on assembly or production line require path planning, i.e. programming the movement of joint angles as function of time. Also through feedback control path tracking is also done to avoid the collision on line. The best way to do so is first configure the path geometrically and then derive it as time dependent function. Obstacle avoidance has been achieved by formulating state constraints with optimal-control. Distance between the colliding parts is considered as the constraints. These constraints are considered as function depending on position of system that is not differentiable continuously. Therefore, the distance function is modelled as convex set thus making them continuously differentiable. The algorithm proposed is standard minimization using convex modelling of constraints [**7**].

The gaits which use pair of legs in quadruped robot like trot, pace and bound were explored, In trot gait diagonal pairs were used , in pace lateral pairs and front-rear pairs in bound gait are used. It was found that pairs can be considered as one leg and an algorithm for virtual biped can be developed for all three gaits. Thus, this algorithm is implemented on quadruple robot and is found experimentally valid. The algorithm controls the jumping height, forward motion and body attitude [**8**].

Turning gait was proposed while controlling the attitude and linear movements simultaneously. First, the feasible sequence of leg movement was found. Among the entire gaits, feasible gait is selected. In addition, the posture of robot while moving is studied where the center of gravity should always stay inside the polygon formed by the legs on ground. The gait used for turning moves one leg at a time [**9**].

Optimal gait for quadruped reduces the energy required by the actuators for walking.
By varying leg motion, ground contact and liftoff time various gaits can be achieved. Here hybrid optimal control is used for finding the feasible gait [**10**].

The walking of a biped for uneven and inclined surface has been discussed. An algorithm walking control was described for biped robot walking on inclined surface. Previously without considering the global and local inclination of floor for designing the controller, it worked well for flat surface and slight inclined floor but as inclination increases the robot fells down. Thus, six online controllers are added for controlling the jerk from ground, step timing and angular momentum [**11**].

The robot named Little Dog uses two level planner controller: high level controls the path planning, i.e. the placement of footsteps in given terrain, whereas low level controller does path tracking using closed loop system [**12**].

For the bounding gait, a planning algorithm is discussed. Bounding gait is a dynamic gait thus it cannot be planned using approximations be unlike the walking gait. Linear Quadratic Regulator is used for controlling the bound gait. The robot used for experimentation was Little Dog [**13**].

The robots like Little Dog and Big Dog do not have body that is flexible. It is seen in four legged robots that flexibility in their body increases their agility. The study's aim was to observe how stability and walking energy efficiency in trot, bound and step climbing is effected by flexibility of body. It was found that the flexibility increases energy efficiency. In addition, it increases the height of raising the robot; it's speed and foot clearance. Thus, it provides increased speed and enhanced mobility [**14**].

The initial research was done on mechanical design and its configuration, during which it increase the flexibility of actuator elastic joints were designed, which help the robot to acclimatize with its surroundings easily. Use of elastic joints in actuators increases their area of application. They have high portability and can be used where soft driving is required [**15**].

Walks are divided into two classes, i.e. static walk and dynamic walk. Dynamic walk is desirable because of higher speed and less energy consumption. The three criteria for analyzing the superiority of gait is: speed, energy consumption and stability. The relation between these criteria's is concluded as (i) for stability the step size should be small, (ii) for maximum speed the step size should be wide, (iii) trot gait is desirable for better energy consumption, whereas pace gait for more speed [**16**].

2.1.3 Literature Review on Bond Graph Modelling Technique.

The Bicycle model is discussed here to understand the kinematics of vehicle model for easy understanding. It clearly shows the relations how the vehicle body moves due to the rotation of wheels. The modelling is done through bond graph technique. A bond graph for a four-wheel vehicle model is also presented. The traction forces from ground act on the wheels pushing it to move forward. The steering and anti-braking system is incorporated in the bond graph models. The steering mechanisms provides turning in motion [**17**].

The parameter defining the stability control in particular cases were studied. There is a separation between stable and unstable zones in the range of dynamic system using mathematical conditions. Stable zone's separation property is described mathematically as dynamic system. Mathematical model of a robot walking in unpredictable terrain is applied in highly dynamic system [**18**].

A three dimensional model of quadruple robot has been modelled in bond graph. Trot gait for straight path and amble gait for turning was implemented. Trot gait was found to be more energy efficient then amble gait. The minimum lift to leg for increased energy efficiency and maximum length was achieved for maximum speed [**19**].

2.2 Observations from Literature

It is observed from the extensive literature survey that a lot of work has been carried out in the field on legged robots. Scientists have shown simulations for various gaits and different mechanical configuration of the legged robots. In fact, the mentioned parameters have been connected to measurable parameters a number of times using a number of techniques. Bond graph modelling technique has also not only been applied successfully on many occasions but has brought revolutionary conclusions also. However, this particular section of modelling a legged robot as a planar model has not been the paragon of focus for bond graph modelers. So, it was decided to further extend the work in modelling first the model as a two-legged planar model. Thus, further implementing its results in modelling of quadruple model have planar model as its basis. Further in three-dimensional model, the leg of the quadruple as taken inspiration from model of wheel in bond graph [**17**]. The modelling of a leg in such way has not been done by any technique so far.

2.3 Objective of Present Research

The objective of the present work is as follows:

- Modelling of a two-legged planar model. For modelling, we will first model the links of leg that will be joined to form complete leg.
- Taking basis from two-legged robot a quadruple robot will be modelled.
- An alternative three-dimensional model will be modelled. For modelling, the same bond graph for body and legs will be made.
- Then simulation will be run for various gaits for finding the most energy efficient gait.

Chapter 3

Planar Model of Two-Legged Robot

This chapter gives the comprehensive account about modelling of two-legged robot's planar model and its bond graph based modelling. The modelling and simulation are done in Symbols Shakti 2.0 software environment. The graphs distinctly show the locomotion of robot by varying the power supply to its legs.

3.1 Introduction

The planar model here is a two-legged model that has taken its inspiration from the bicycle model of vehicle. Here, the two legs at the rear and front each of four-leg model are combined together to make a virtual biped. The logic behind doing this was to develop an algorithm for the virtual biped that can be further used for development of quadruple robot. The planar model only considers the lateral, longitudinal and yaw motion of the body.

In this model, control strategy is to balance the lateral and longitudinal motion for making the robot to move forward in a straight path. The graphical representation of planar model is shown in Fig. 3.1. The model body is considered to be a rectangular platform with three degrees-of-freedom in longitudinal direction (x), lateral direction (y) and rotation about vertical z-direction (ψ). The legs consist of two Links having a DC motor attached to each Link. The legs have two degrees-of-freedom i.e. the rotation of both the Links in transverse y-direction (β). The Link1 is attached to the body and the Link2 has contact with the ground.

Here, the control parameter for manipulating the locomotion of model is rotation of the Links of legs and the traction force acting on the Link2 due to contact with the ground. Due to the traction force provided by the ground the robot moves forward. The manoeuvres of the leg can be controlled by varying the supply of power to its motors of its Links.

Thus, for modelling the planar model, it is first needed to model its legs and also, the joint rotation of Links for the desired motion. In the following section, the modelling of legs, its joint rotation and different models based on the basic model have been described in detail.

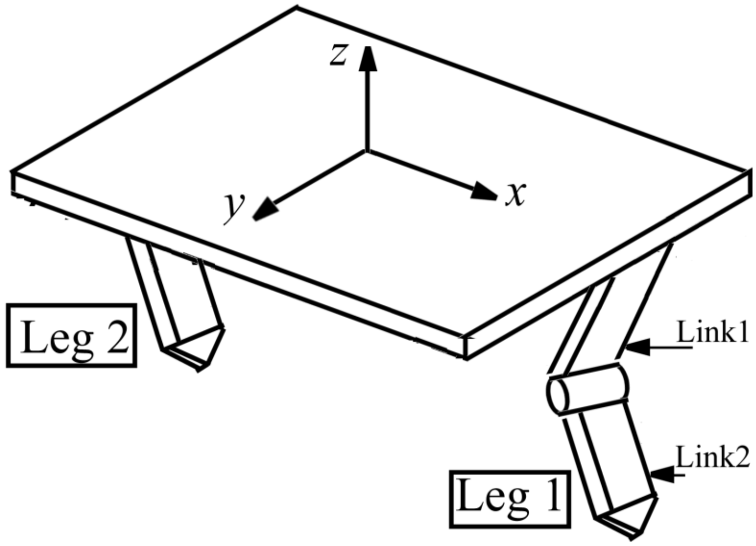

Fig. 3.1 Schematic representation of 2- legged planar model

3.2 Modelling of Planar Model using Bond Graph

The initial step for modelling of planar model is modelling of its legs. The modelling of legs needs special attention, as they are the ones that control the forward motion of robot as well as the different manoeuvres of motion. Different gaits are also achieved by coordinating the movement of the legs in a certain manner. The legs here have two degrees-of-freedom i.e. rotation of each Link about y-direction (β) . The first Link transfers its rotation to second Link, further second Link has its own rotation also and the traction force acts on it due to its contact with the ground. In this section, discussion is on the modelling of Links and then final modelling of complete leg.

3.2.1 Modelling of First and Second Link of Leg

Each Link is considered as a spring-mass-damper system that gets its power supply from a DC motor connected to each Link. The current supply to the motor is modulated in such a way that it gives the desired locomotion to the legs. Here, in modelling the Links the most important aspect is that the modulated power is supplied to the Link in desired form for the accurate movement of Links.

As explained in bond graph approach compliance element C is an integrating element. Thus, whatever supply is given to the motor is getting integrated before being supplied to the Link. Thus, it is required to differentiate the power supply at two places so that the power supply does not get integrated. Bond graph for both the Link is same as shown in Fig. 3.2.

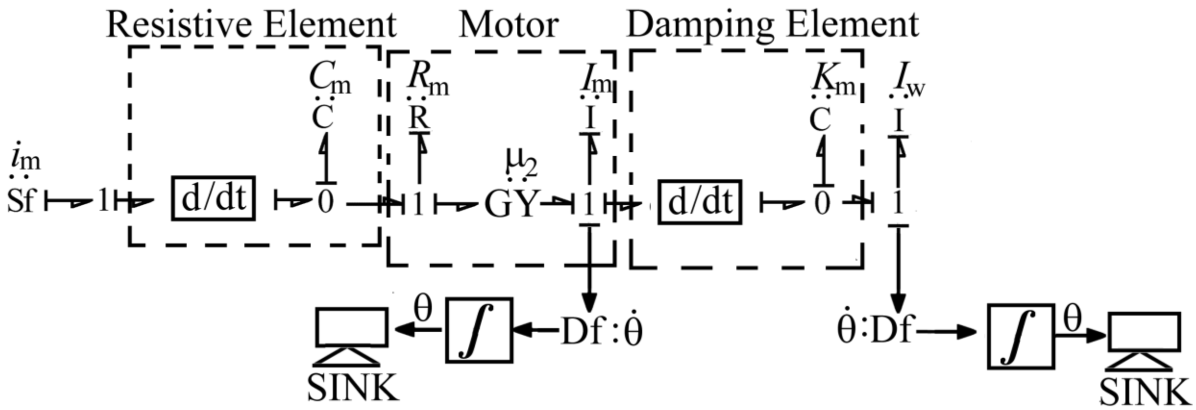

Fig. 3.2 Bond graph model of a single link of leg

The Sf-element here represents the input current i_m to the motor for rotation of legs. As the input is given as polynomial, it will be integrated by the C-element and thus, there is need to add a differentiator for getting the original input. The differentiator di_m/dt differentiates the input and gives it to capacitor C_m that is parallel to Sf-element that is an energy-storing element. The differentiator along with the capacitor connected at 0-junction is equivalent to electrical resistance. The effort (voltage) from 0-junction is then passed to resistance R_m that is in series with gyrator element GY having modulus of μ_2. The gyrator element GY converts the flow into effort i.e. the current to torque.

The 1-junction to which I-element and flow sensor Df is connected represents rotor speed of motor. Here, I_m is the mass moment of inertia of the motor. The sensor Df senses the angular velocity $\dot{\theta}$ of rotor and then integrates it by an integrator $\int$ and thus, gives it angular position. To convert the angular velocity into effort input for Link a 0-junction is added with compliance element K_m. But, since K_m is an integrator element there is need to differentiate the angular velocity. Thus, differentiator $d\theta/dt$ is added before K_m. the differentiator along with the stiffness connected at 0-junction is equivalent to mechanical damping. Thus, the effort torque received goes to 1-junction to which an inertial element and flow sensor is attached. I_m is mass moment of inertia of leg and the flow sensor gives angular velocity of leg.

3.2.2 Modelling of Full Leg

Once both the Links are modelled, they are joined together by a joint stiffness to frame the complete model of a leg. The bond graph for the full leg model is shown in Fig. 3.3.

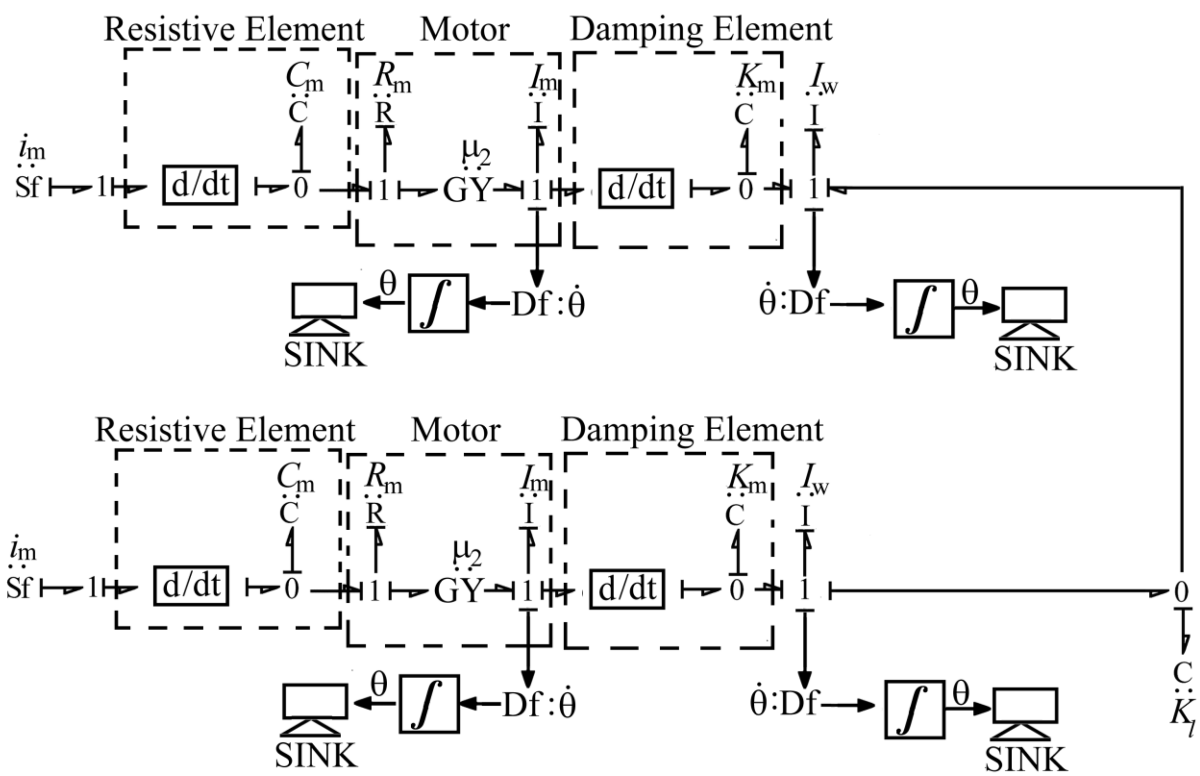

Fig. 3.3Bond graph model of complete leg

The Sf-element here represents the input current i_m to the motor for rotation of legs. As the input is given as a polynomial it will get integrated by the compliance element Thus, there is a need to add a differentiator for getting the original input. The differentiator dV_m/dt differentiates the input and gives it to capacitor C_m which is parallel to Sf-element which is an energy storing element. The effort from 0-junction is then passed to resistance R_m which is in series with gyrator GY. The gyrator GY converts the flow to effort i.e. the current flow to torque. The 1-junction to which I_m and flow sensor Df is connected represents rotor of motor. Here, I_m is the mass moment of inertia of motor. DF senses the angular velocity $\dot{\theta}$ of rotor and then integrates it by an integrator $\int$ and thus, gives it angular position.

To convert the angular velocity into effort input for Link addition of 0-junction with compliance element K_m is done. But since K_m is an integrator element there is need to differentiate the angular velocity. Thus, there is addition of differentiator $d\theta/dt$ before K_m. Thus, the effort received goes to 1-junction to which an inertial element and flow sensor is attached. I_m is mass moment of inertia of leg and the flow sensor gives angular velocity of leg. This explanation holds good for both Links and they are then further attached to the by 0-junction which has compliance element (joint stiffness) K_l attached to it. This junction converts the angular velocity of Link1 to effort and transfers it to Link2 and vice versa. Thus, both Links are joined together to form a complete leg, thus, transmitting the desired locomotion of leg.

3.3 Joint Rotation for Development of Motion

The joint rotation of both the Links is an important aspect of modelling of legs. It has been observed that in locomotion of animals, the first Link that can be considered as thigh connected to the body always moves forward, whereas the lower Link of leg first goes backward and then moves forward. Both the Links reach their maximum angular movement in same time and then together move down. To achieve the same mathematical formulations and programming is required to achieve the motion that is explained in the sections below:

3.3.1 Mathematical Formulation for Desired Motion of Robot.

As explained above to achieve the desired motion for both the Links, a mathematical formulation is required. While deriving the mathematical formulation, requires four different motions of leg at a given time. The reason for the same is that there will be a phase difference between the legs, when one leg will come down the other will start rising from the ground to keep the movement going. Thus, each Link will have two formulations each for accommodating the phase difference while moving. The desired motion of Links are graphically represented in Fig. 3.4.

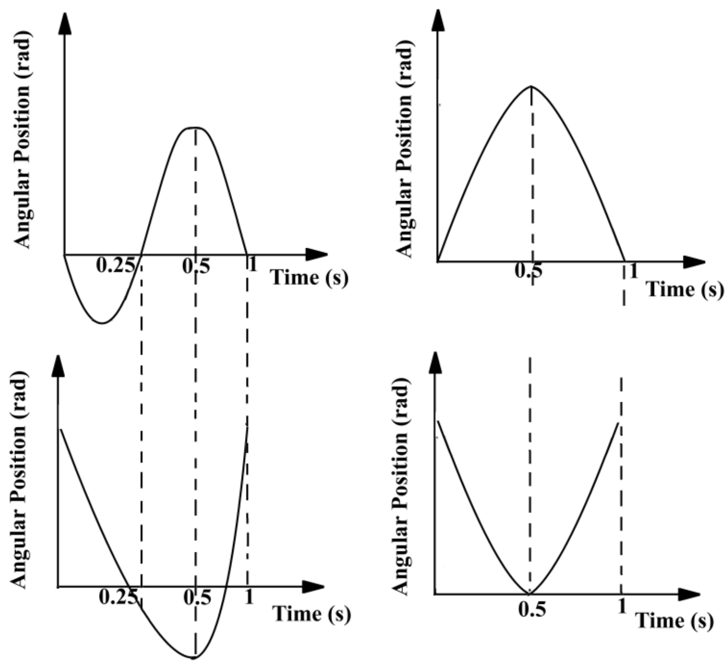

Fig. 3.4(a) Motion of Link1 and (b) Motion of Link2 in first and second step

The Fig. 3.4(a) shows the phase difference between first and second step of Link1. It clearly depicts that when the Link1 of first leg is at its peak angular position the Link1 of second Link is at ground. Similarly, Fig. 3.4(b) shows the phase difference between first step and second step of Link2.

A four-degree polynomial has been derived to achieve the desired results

$$\theta(t) = a_1 t^4 + a_2 t^3 + a_3 t^2 + a_4 t + a_5 \tag{3.1}$$

Thus, it is assumed that $\theta(0) = \theta_0, \theta(0.25) = \theta_1, \theta(0.5) = \theta_2, \theta(0.75) = \theta_3, \theta(1) = \theta_4$ and putting above values in Eq. 3.1,

$$\theta_0 = a_5 \tag{3.2}$$

$$\theta_1 = a_1(0.25)^4 + a_2(0.25)^3 + a_3(0.25)^2 + a_4(0.25) + a_5 \tag{3.3}$$

$$\theta_2 = a_1(0.5)^4 + a_2(0.5)^3 + a_3(0.5)^2 + a_4(0.5) + a_5 \tag{3.4}$$

$$\theta_3 = a_1(0.75)^4 + a_2(0.75)^3 + a_3(0.75)^2 + a_4(0.75) + a_5 \quad (3.5)$$

$$\theta_4 = a_1 + a_2 + a_3 + a_4 + a_5 \quad (3.6)$$

Writing the above equations in matrix form,

$$\begin{bmatrix} 0 & 0 & 0 & 0 & 1 \\ 0.25^4 & 0.25^3 & 0.25^2 & 0.25 & 1 \\ 0.5^4 & 0.5^3 & 0.5^2 & 0.5 & 1 \\ 0.75^4 & 0.75^3 & 0.75^2 & 0.75 & 1 \\ 1 & 1 & 1 & 1 & 1 \end{bmatrix} \begin{bmatrix} a_1 \\ a_2 \\ a_3 \\ a_4 \\ a_5 \end{bmatrix} = \begin{bmatrix} \theta_0 \\ \theta_1 \\ \theta_2 \\ \theta_3 \\ \theta_4 \end{bmatrix} \quad (3.7)$$

Thus,

$$\begin{bmatrix} a_1 \\ a_2 \\ a_3 \\ a_4 \\ a_5 \end{bmatrix} = \begin{bmatrix} 0 & 0 & 0 & 0 & 1 \\ 0.25^4 & 0.25^3 & 0.25^2 & 0.25 & 1 \\ 0.5^4 & 0.5^3 & 0.5^2 & 0.5 & 1 \\ 0.75^4 & 0.75^3 & 0.75^2 & 0.75 & 1 \\ 1 & 1 & 1 & 1 & 1 \end{bmatrix}^{-1} \begin{bmatrix} \theta_0 \\ \theta_1 \\ \theta_2 \\ \theta_3 \\ \theta_4 \end{bmatrix} \quad (3.8)$$

Thus, by using the values from Table 3.1 and solving the Eq. 3.1 in Matlab software the values of a_1, a_2, a_3, a_4, a_5 are obtained. Thus, the following four equations are obtained:

$$\text{SF1} = -4.1045(t)^4 + 6.3509(t)^3 - 3.1115(t)^2 + 0.8651(t) + 0.1047 \quad (3.9)$$

$$\text{SF2} = 1.8198(t)^4 - 16.2177(t)^3 + 20.0207(t)^2 - 5.6228(t) + 0.1047 \quad (3.10)$$

$$\text{SF3} = 4.4651(t)^4 - 6.8821(t)^3 + 3.2073(t)^2 - 0.7903(t) + 0.3839 \quad (3.11)$$

$$\text{SF4} = 21.7451(t)^4 - 36.2261(t)^3 + 19.3993(t)^2 - 4.9183(t) + 0.8832 \quad (3.12)$$

Where, SF1 and SF3 are power supply to the motor for first Link for first and second step, respectively; SF2 and SF4 are power supply to the motor for second Link for first and second step, respectively.

Table 3.1 Joint rotation for motion

Time Period	Link1 First step Angles (θ)	Link2 First Step Angles (θ)	Link1 Second Step Angles (θ)	Link2 Second Step Angles (θ)
$t = 0$	0.1047	0.1047	0.3839	0.8832
$0 < t \le 0.25$	0.2097	-0.2960	0.2967	0.3850
$0.25 < t \le 0.5$	0.2967	0.3850	0.2094	0.1047
$0.5 < t \le 0.75$	0.3839	0.8832	0.1047	-0.2960
$0.75 < t \le 1$	0.1047	0.1047	0.3839	0.8832

3.3.2 Development of Program for Continuous Motion

After developing the mathematical formulation the next step was that, the robot follows this motion as long as it wants to move. As the above formulation has each step for 1 sec, it is desired that each step should repeat itself after competition of each step. Thus, after mathematical formulation it is required to program the motor input so that it keeps on repeating itself until the supply is stopped.

Let time period for each step $= T$ and Time period for which simulation is run $= t$

Thus, for programming

$$T = 1 \tag{3.13}$$

$$T1 = t \tag{3.14}$$

$if\ T < T1$

$$\text{No of rotations, n} = \frac{T1}{T} \tag{3.15}$$

$$T = T1 - T \times n \tag{3.16}$$

Else $T = T1$ and

$$SF = a_1 T^4 + a_2 T^3 + a_3 T^2 + a_4 T + a_5 \tag{3.17}$$

Thus, the above polynomial will repeat it after completion of each step. The values of a_1, a_2, a_3, a_4, a_5 have already been found in the above section.

3.3.3 Bond graph Simulation of Leg Exhibiting Desired Motion

In Fig. 3.5, it is shown that the simulation of the leg is exhibiting the desired motion run for 10 s. The parameters used in simulation are given in Table 3.2.

Table 3.2Parameter values

Parameters	**Description**	**Values**
C_{m}	Capacitance of motor (F)	10
λ	Differentiability constant	7
I_{m}	Moment of inertia of motor (kg m^2)	1
I_{w}	Moment of inertia of leg (kg m^2)	5
$K_{\mathrm{m_{f1}}}$	Compliance element of Link1 $(\mathrm{N/m})$	10^8
K_{l}	Compliance element of leg's $(\mathrm{N/m})$	10
$K_{\mathrm{m_{f2}}}$	Compliance element of Link2 $(\mathrm{N/m})$	10^7
R_{m}	Resistance of motor (Ω)	0.1
μ_1	Modulus of Gyrator for motor of Link1	0.7
μ_2	Modulus of Gyrator for motor of Link2	1.95

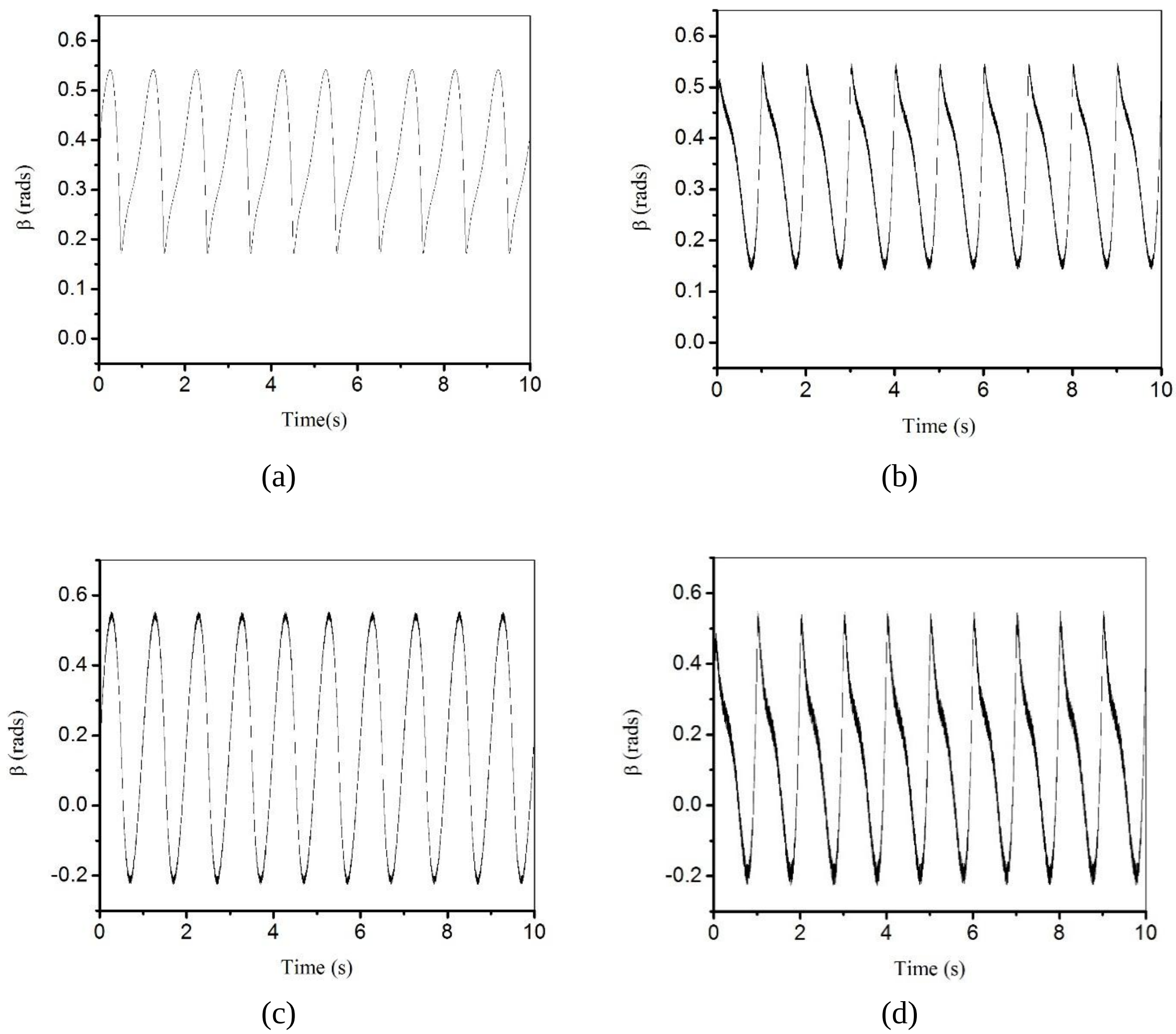

Fig. 3.5(a) Angular movement of step 1 of Link1 (b) Angular moment of step 2 of Link1 (c) Angular moment of step 1 of Link2 (d) Angular moment of step 2 of Link2

It is a simulation run only for leg until the leg has not yet been attached to the body. The Fig. 3.5(a) shows the angular position of Link1 of leg1 that takes the first step. It reaches the maximum amplitude of 0.54 rad from its initial position. The Fig. 3.5(c) shows the angular position for Link1 of leg2 that will take second step. Thus, it can be clearly seen from the results that mathematical formulation is giving correct results and the program is exhibiting the continuous motion. In addition, it can also be clearly seen that there is phase difference between the two steps. Fig. 3.5(b) shows the angular position of Link2 of leg1 that takes first step. It can been seen clearly that the Link2 first goes backward and then reaches peak amplitude of 0.54 rad in same time as that of Link1. Fig. 3.5(d) shows the angular position of Link2 of leg2 moving second step. It can be see that there is phase difference with leg1 and that it reaches its maximum amplitude in same time as the Link1 of its leg.

3.4 Development of Different Models in Bond Graph

After the modelling of all the sub models required and mathematical formulations done, the modelling of the complete planar model is done. Before starting the modelling, it is required to study the kinematic relations. In this section, the discussion is on the kinematic relations and different models using these kinematic relations using bond graph.

3.4.1 Kinematic Relations

The kinematic relations discussed here constitute the main part of the model [17]. From these relations, the rotations of legs, lateral and longitudinal movement of body are incorporated in the model.

The front leg's velocities which are normal and tangential to the rotation axis are

$$v_{1n} = (v + \omega l_1)\cos\delta - u\sin\delta \tag{3.18}$$

$$v_{1t} = (v + \omega l_1)\sin\delta + u\cos\delta \tag{3.19}$$

The rear leg's velocities which are normal and tangential to the rotation axis are

$$v_{2n} = (v - \omega l_2) \tag{3.20}$$

$$v_{2t} = u \tag{3.21}$$

From Newton Euler equations

$$m_v \dot{u} = m_v \omega v + \sum F_x \tag{3.22}$$

$$m_v \dot{v} = -m_v \omega u + \sum F_y \tag{3.23}$$

3.4.2 Bond graph model of Planar Model with Single Link

Modelling the planar model using the above kinematic relations, the model as shown in Fig. 3.6 is achieved.

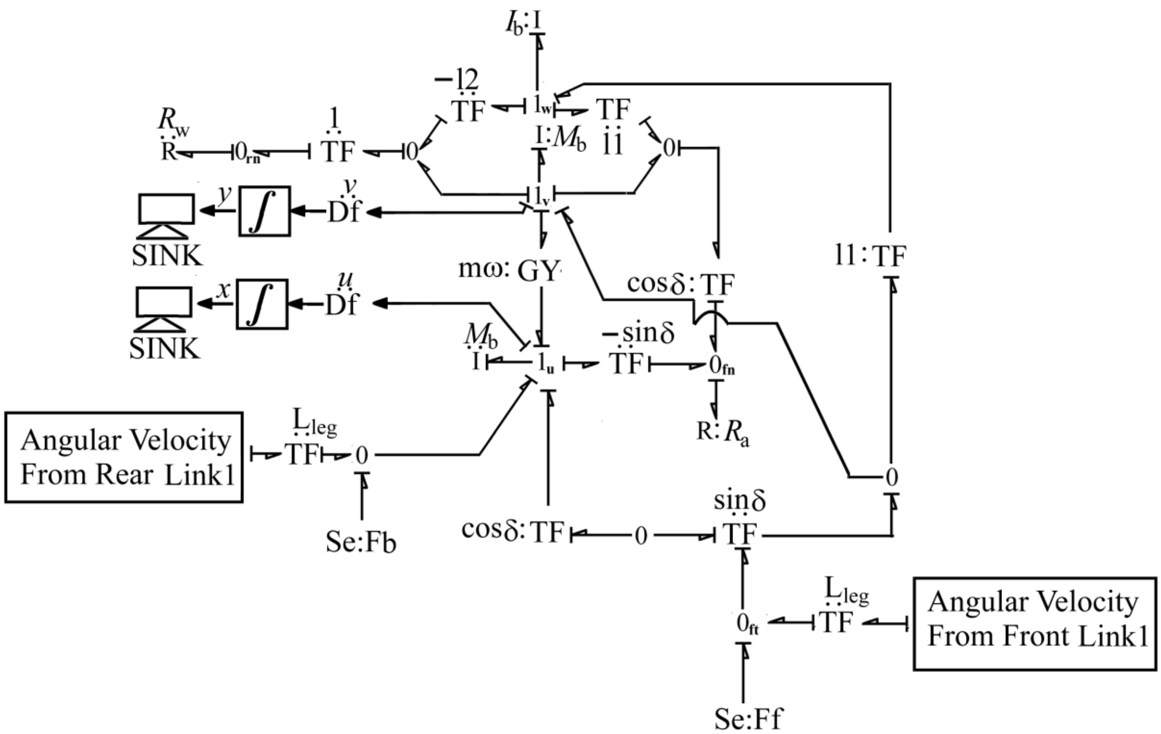

Fig. 3.6 Bond graph model of planar model with single Link

The Sf here represents the input current i_m to the motor for rotation of legs. As input is in polynomial form it will get integrated by the compliance element thus, addition of a differentiator for getting the original input is done. The differentiator di_m/dt differentiates the input and gives it to capacitor C_m which is parallel to Sf which is an energy storing element. The effort from 0-junction is then passed to resistance R_m which is in series with gyrator GY. GY converts the flow to effort i.e. the current flow to torque. The 1-junction to which I_m and flow sensor Df is connected represents rotor of motor. Here I_m is the mass moment of inertia of motor. Df senses the angular velocity $\dot{\theta}$ of rotor and then integrates it by an integrator $\int$ and thus, gives it angular position. To convert the angular velocity into effort input for Link addition of a 0-junction with compliance element K_m is done. But since K_m is an integrator element it is required to differentiate the angular velocity. Thus, a differentiator $d\theta/dt$ is added before K_m. Thus, the effort received goes to 1-

junction to which an inertial element and flow sensor is attached. I_m is mass moment of inertia of leg and the flow sensor gives angular velocity of leg.

Here in this model, 1_u, 1_v, and 1_ω represent the longitudinal, lateral and angular velocity of center of gravity of body. Thus, the angular velocity of leg is sent to transformer TF with modulus value L_{leg} and longitudinal velocity is calculated. Se: Fb and Se: Ff represent the traction force which is being applied on Link2 due to the traction force acting on it. It sums up at 0-junction that is then transferred to 1_u to get velocity v_{2t}. The above explanation is for rear legs. For front legs, the connections are same until traction force acts on it. After that v_{1t} as represented in Eq. 3.19 is achieved. δ is the turning angle for the legs in front. In this model, turning is considered only in front side.

A gyrator GY with modulus m_ω to accommodate the forces acting on body due to its movement in its various directions. Eq. 3.18 and 3.20 are incorporated using transformers TF with modulus l_1,-l_2, cosδ, sinδ and –sinδ. The inertial element connected I_ω is mass moment of inertia of body, whereas M_b is mass of body. The sensors are attached to velocity ports of u, v and ω to detect the velocities of these ports.

3.4.3 Bond graph of Planar Model with Complete Leg

The bond graph of planar model in Fig. 3.6 with complete leg is extension of previous model. Here, the complete leg with both the Links have been incorporated in the model. The only addition in this model is of joint between the two Links which is represented by compliance element K_l. Also, the GY values of μ_1, μ_2, μ_3 and μ_4 are introduced for the motors of the four Links.

3.5 Parameter Values and Simulation Results

In this section, the parameter values and simulation results for the planar model are discussed. These parameters lead to the basis for developing the quadruple model. Table 3.3 contains the parameters. The results discussed in this section prove that the kinematic relations and mathematical formulation discussed in previous sections are of relevance with the model.

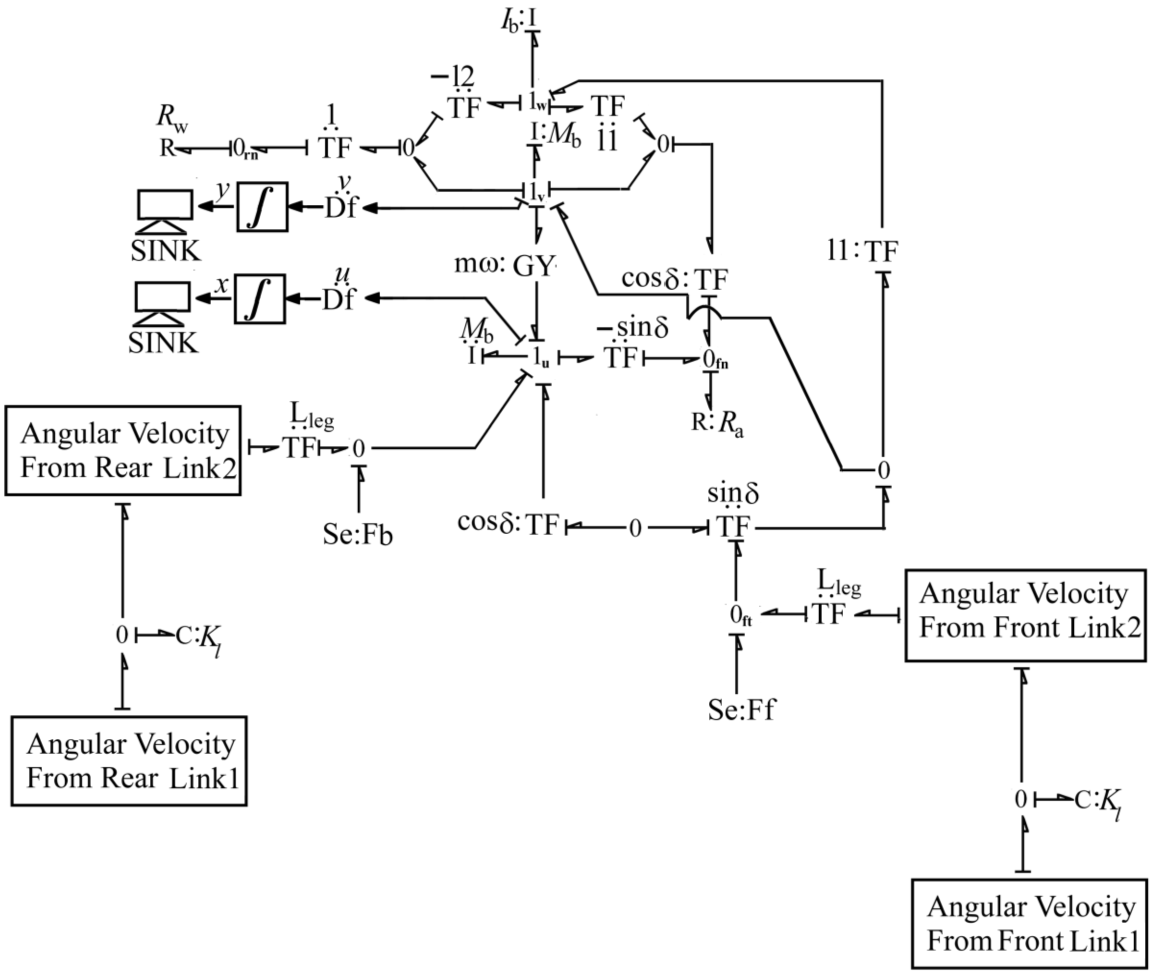

Fig. 3.7 Bond graph of planar model with complete leg

Table 3.3 Parameter values

Parameters	**Description**	**Values**
C_m	Capacitance of motor (F)	10
λ	Differentiability constant	7
I_m	Moment of inertia of motor (kg m^2)	1
I_b	Moment of inertia of body (kg m^2)	10
I_w	Moment of inertia of leg (kg m^2)	5
$K_{m_{f1}}$	Compliance element of front leg's Link1 (N/m)	10^8
K_l	Compliance element of leg's (N/m)	10

$K_{m_{f2}}$	Compliance element of front leg's Link2 $(\mathrm{N/m})$	10^7
$K_{m_{r1}}$	Compliance element of rear leg's Link1 $(\mathrm{N/m})$	10^8
$K_{m_{r2}}$	Compliance element of rear leg's Link2 $(\mathrm{N/m})$	10^6
L_{leg}	Length of complete leg(m)	0.6
l_1, l_2	Distance of front and rear wheel from COG(m)	0.5
M_{b}	Mass of body (kg)	600
R_{m}	Resistance of motor (Ω)	0.1
μ_1	Modulus of Gyrator for motor of front leg's Link1	2.1
μ_2	Modulus of Gyrator for motor of front leg's Link2	0.7
μ_3	Modulus of Gyrator for motor of rear leg's Link1	1.95
μ_4	Modulus of Gyrator for motor of rear leg's Link2	0.64

3.5.1 Front and Rear legs with Single Link

The results as shown below are considered from the inception stage of modelling the planar model.

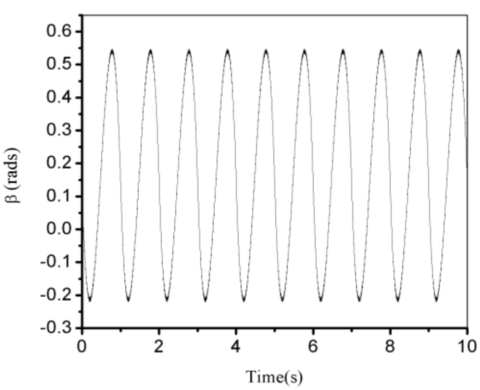

(a)

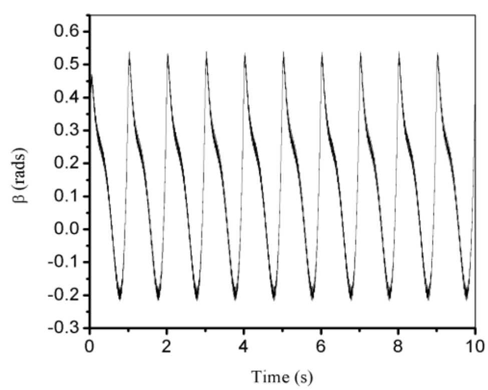

(b)

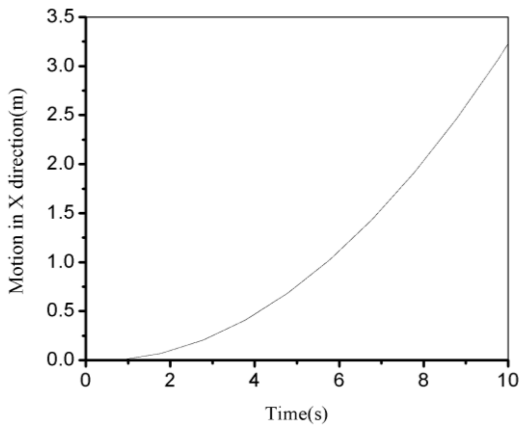

(c)

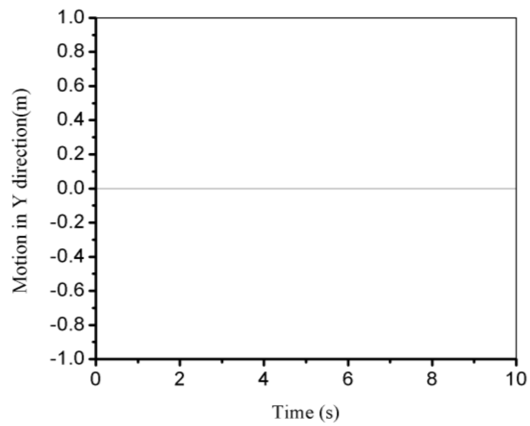

(d)

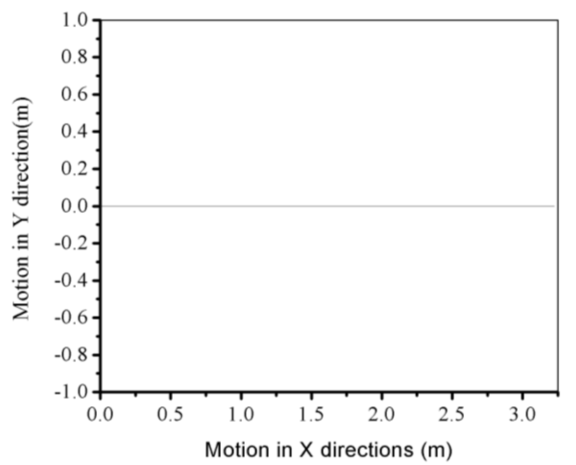

(e)

Fig. 3.8(a) Angular movement of front leg (b) Angular movement of rear leg (c) Motion in x -direction of robot body (d) Motion in y -direction of robot body (e) Motion of robot body in y-direction w.r.t motion in x- direction

Fig. 3.8(a) shows the result for angular position (β) of front leg with single Link w.r.t time. The graph shows that the Link completes one-step in 1 sec and the maximum angular position is 0.54 rad. The input given here is that of Link2. The lowest angular position is -0.22 rad. Thus, the Link2 first goes to its lowest position and then reaches its maximum amplitude.

Fig. 3.8(b) shows the result for rear leg that has the desired phase difference with front leg. Fig. 3.8(c) shows the longitudinal velocity of body developed due to angular velocity of legs. The simulation is run for 10 sec for which body moves 3.25 m i.e. velocity of robot is 0.325 m/s that is an acceptable speed. Also, it can be seen that the body is moving forward and from Fig. 3.8(d) it can be seen that there is no lateral velocity. Thus, the model is stable and moving straight. Fig. 3.8(e) shows the simulation between movement in *y*-direction and *x*-direction which clearly shows that the robot is stable and moving straight.

3.5.2 Front and Rear legs with Two Links

The results for the final planar-model that leads to modelling of quadruple model are discussed in this section. These results also represent that the walking gait by two-legged robot by developing the phase difference between the two legs has successfully been achieved. Also, the robot is walking straight without getting unstable. The desired pattern of angular movement of legs has also been achieved. Fig. 3.8 shows the result for simulation run for the complete planar model.

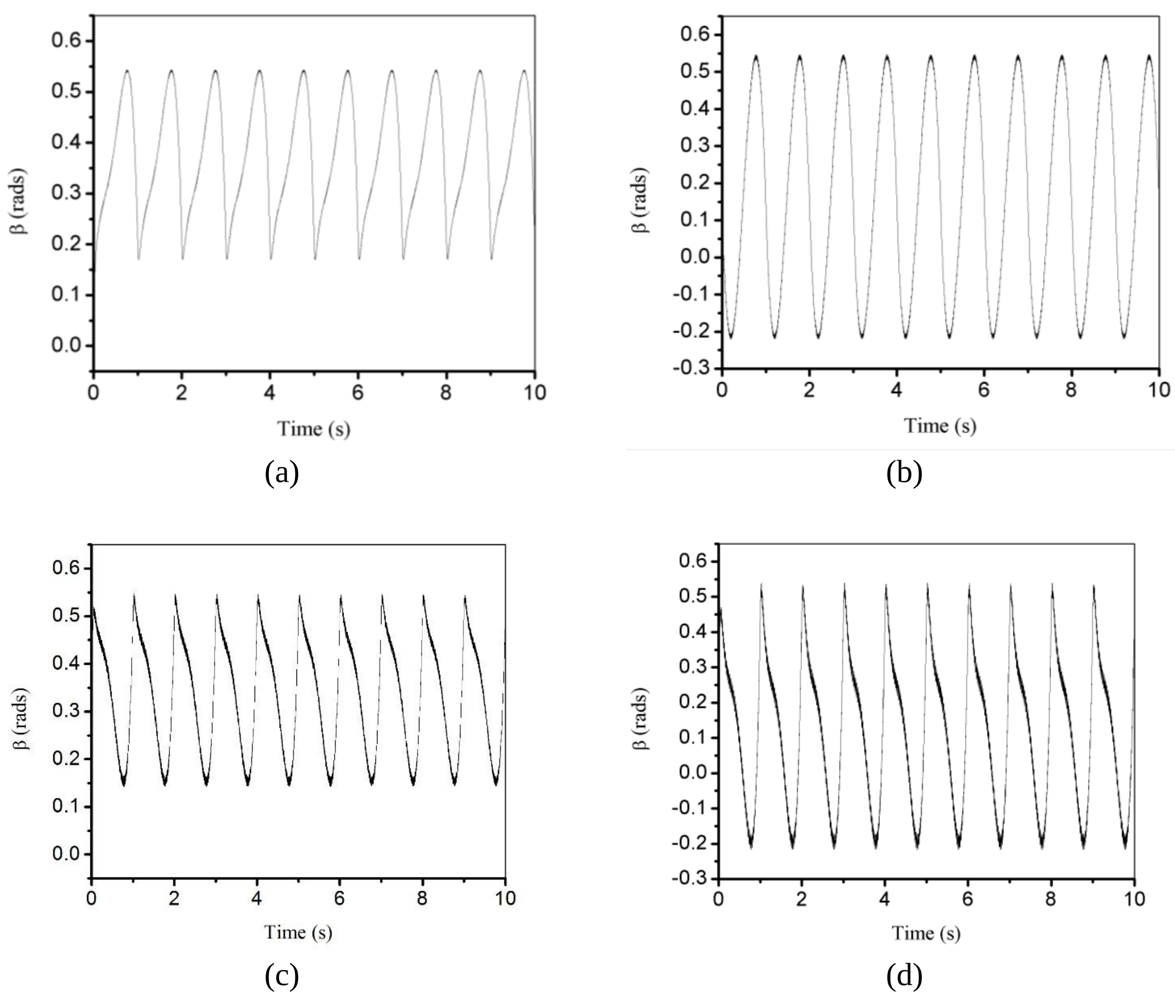

Fig. 3.9(a) Angular movement of front leg's Link1 (b) Angular movement of front leg's Link2 (c)Angular movement of rear leg's Link1 (d)Angular movement of rear leg's Link2

Fig. 3.9 (a) and (c) show the result for the angular position of Link1 (upper) and Link2 (lower) of front leg respectively. It can be seen that the results are according to the mathematical formulation. The maximum amplitude here is also 0.54 rad. Fig. 3.9 (b) and (d) show the result for the angular position of Link1 (upper) and Link2 (lower) of rear leg respectively. It can be clearly seen that the complete model is also giving the desired results.

Fig. 3.10(a) shows the longitudinal distance traversed by the model. It can be seen that the model is moving forward with 0.325 m/s velocity. Also, Fig. 3.10(b) show that there is no moment in lateral direction. Hence, the model is stable and moving forward on straight path. Fig. 3.10(c) and (d) show the results that the phase difference between the Links of front and rear legs has been successfully achieved. It shows that when front legs moves forward the rear leg moves backward. Also it shows that when front leg is at its maximum amplitude the rear leg is at ground maintaining the stability of the model. Thus, these results will act as reference for the results to be achieved in quadruple robot performing different type of gaits.

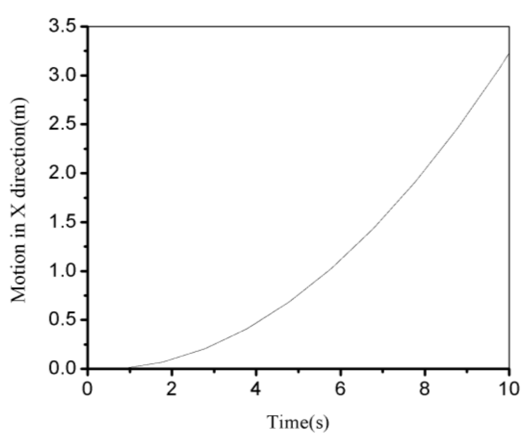

(a)

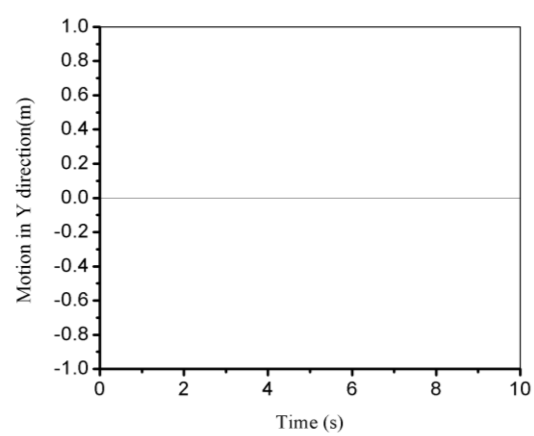

(b)

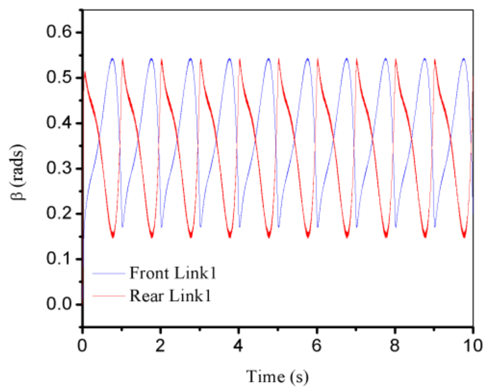

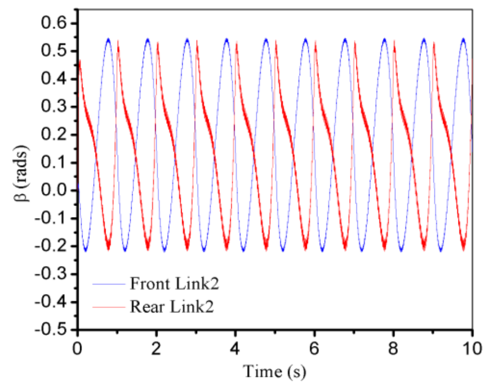

(c) (d)

Fig. 3.10(a) Motion of robot body in *x*-direction, (b) Robot body in *y*-direction, (c) Front leg's Link1 w.r.t rear leg's Link1 and (d) Front leg's Link1 w.r.t rear leg's Link1

Chapter 4

Modelling of Quadruple Robot

This chapter is further extension of work done in Chapter 3, taking the planar model as basis for modelling the quadruple robot and its bond graph. The modelling and simulation are done in Symbols Shakti 2.0 software. The plots distinctly show the locomotion of robot by varying the power supply to its legs.

4.1 Introduction

The quadruple model is a four legged model taking planar model as the basis of modelling. It has been tried to achieve the gaits used by the animals. Though, it is difficult to model the animal's gait completely because it has lot of neural and muscular control. But, there are many manoeuvres which can be done by a robot but not the actual animal. It has been seen in the previous section that the legs are completely following the motion desired.

As the stable walking legged model has already been achieved the strategy for this model is to be able to implement the various gaits. As it has already been discussed about the various gaits in Chapter1, a brief mention for the same is done here to understand their relevance to the quadruple model. A schematic representation of the quadruple robot is shown in Fig 4.1. It is almost like the planar model; just two more legs are added to it. Thus, addition of two legs gives the model the luxury of following the gaits.

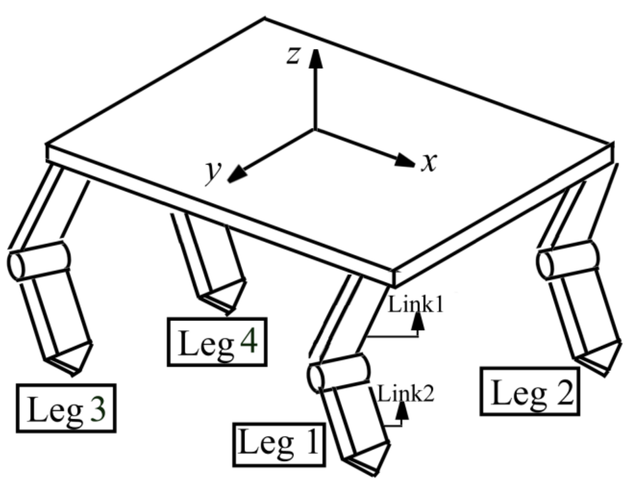

Fig. 4.1 Schematic representation of quadruple model

The gaits are either statically stable or dynamically stable. A statically stable gait provides slow motion to the body and requires balancing of center of gravity of body with each step. In this, the robot moves one-step at a time, the general name for this gait is Amble gait. It has been graphically represented in Fig 1.4 in Chapter 1. The dynamically stability is used for faster motion and they do not require the balancing of center of gravity of the body. In these gaits, two legs move together for achieving the desired gait. Trot, bound and pace are dynamically stable gaits.

Thus, now the kinematic relations will be discussed for modelling of the quadruple robot. Also, an alternative model is achieved which provides more degrees-of-freedom to the legs.

4.2 Development from Planar Model to Quadruple Model

Here in this section, the development of quadruple robot from planar model is discussed. Addition of two more legs adds to some changes in the kinematic relation and as well as in bond graph model. The quadruple robot has the ability to perform various gaits according to the requirement of terrain as well as speed. Further, an alternative model is also proposed with more degrees-of-freedom that follows the dynamically stable gaits. Thus in following section, the kinematic relation and bond graph of proposed models are discussed.

4.2.1 Kinematic Relations

Kinematics is the review of the components of a mechanical system, where the motion is illustrated in form of the velocity and acceleration of its components. The components can be joined through various types of joints, thus constraining movement of components with respect to each other. Newtonian mechanics illustrates that the forces which act on a system can modify the motion of the system. The forces can be classified into two types (i) the constraint forces that constrain the motion, (ii) the generalized forces that cause the motion. Kinematics does not consider constraint forces while describing the connections and constraints produced by them. Also, it does not consider generalized forces while defining the motion of joined components.

Each component of the mechanical system is assumed a rigid body. A rigid body is one in which the parts of a component does not move relative to each other. The geometry of the system can be represented by the coordinate system. Thus, by specifying the coordinates the specification of a mechanism can be known. The coordinates are selected according either to the position of components or for simplifying the equations. The minimum number of coordinates that define the structure of the system is known as degrees-of-freedom. A kinematic motion of the system is defined by making its coordinates function of a particular variable, for example time, and thereby generating a curve for the motion of all points in the mechanism. The coordinates are specified according to the frame they are in e.g. body fixed frame which is with reference to the system itself and inertial frame which is in reference with earth. The body fixed frame moves with the body i.e.it will move relative to inertial frame, whereas the inertial frame is fixed.

The concentration is on the forward kinematics, which is that by using coordinates of system it can be configured. This is generally a simple problem that the coordinates chosen for defining the system are function of a variable.

The kinematic relation discussed here are similar to that of planar model with addition of angular velocity ω in equations. From these relations the motion of at center of gravity of body is deduced when the robot is moving with its four Legs.

The front leg's velocities that are normal and tangential to the rotation axis are

$$v_{1n} = (v + \omega l_1)\cos\delta - u\sin\delta \tag{4.1}$$

$$v_{1t_L} = (v + \omega l_1)\sin\delta + u\cos\delta - c\omega \tag{4.2}$$

$$v_{1t_R} = (v + \omega l_1)\sin\delta + u\cos\delta + c\omega \tag{4.3}$$

Where v_{1t_L} =Leg 1(front left leg), v_{1t_R} =Leg 2(front right leg), c =distance of legs from COG of body in y-direction.

The rear leg's velocities that are normal and tangential to the rotation axis are

$$v_{2n} = (v - \omega l_2) \tag{4.4}$$

$$v_{2t_L} = u - c\omega \tag{4.5}$$

$$v_{2t_R} = u + c\omega \tag{4.6}$$

Where v_{2t_L} $=$Leg 3(rear left Leg), v_{2t_R} $=$Leg 2(rear right Leg).

From Newton Euler equations

$$m_v\dot{u} = m_v\omega v + \sum F_x \tag{4.7}$$

$$m_v\dot{v} = -m_v\omega u + \sum F_y \tag{4.8}$$

4.2.2 Bond Graph Model

As the kinematic relation has been deduced in previous section based on them the bond graph for the model has been made as shown in Fig. 4.2. The ports inside circle (1, 2, 3, and 4) represent the Legs of the robot. The bond graph for the same has been shown in Fig. 3.3 in Chapter 3. The angular velocities from the Legs go to TF having modulus L_{Leg} which gives us linear velocity of leg. As quadruple model has four Legs the linear velocity due to angular movement of body is also to be considered. Thus, the angular velocity from 1_ω is given to TF with modulus value 'A' for right side legs and '–A' for left side legs according to geometry of robot. The effort is required at junction 1_u so a 1 junction is added with compliance element K_l after 0 junction where traction force is acting. The effort from 1 junction sums up at 0 junction with the effort coming from 1_ω junction and goes to 1u. The sensors Df are attached to 1_u, 1_v and 1_ω to measure the velocities as well as position of the center of body.

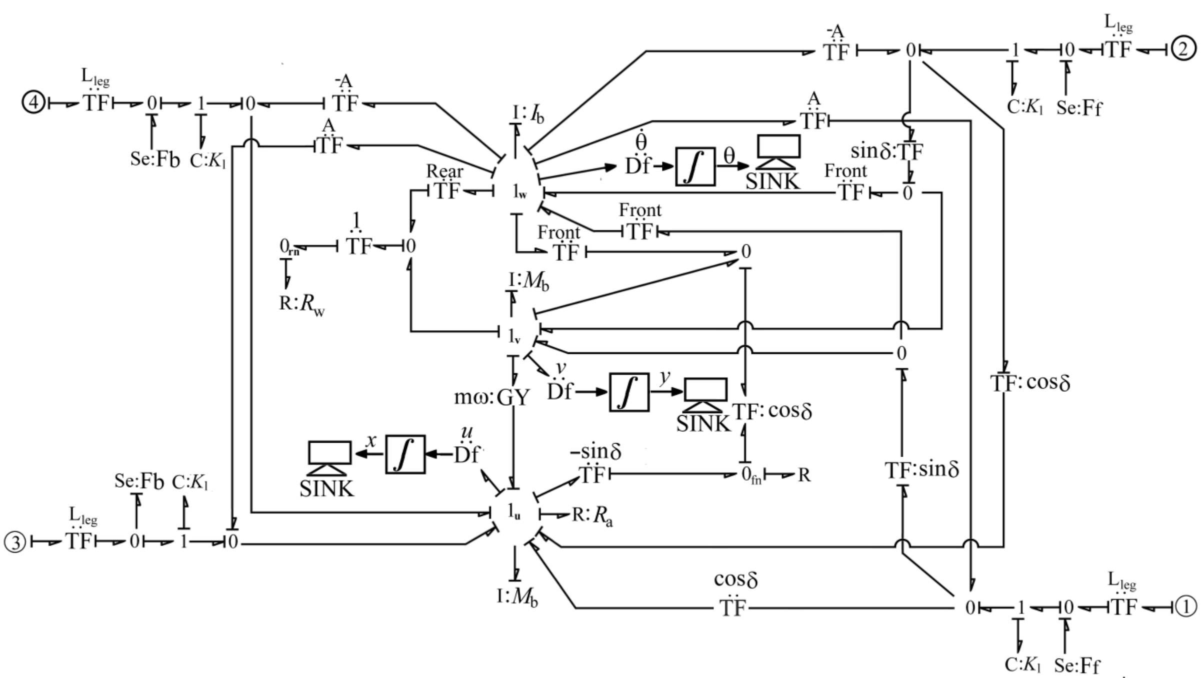

Fig. 4.2 Bond graph of quadruple robot

4.3 Alternative Model using Three-Dimensional Model

Here, an alternative model for quadruple robot has been developed which is a three dimensional dynamic model using bond graph technique. The Leg and robot body's bond graph are discussed in this section. For dynamic stability of the robot turning motion at different speeds is studied. The study is also beneficial for managing different gaits.

4.3.1 Kinematic Relations

It is assumed that the quadruple robot is balanced along its longitudinal axis. Spring-damper system is used to represent joints between the Links, also acting as energy storing and dissipating elements allowing rotation along y-direction (β) of the Links.

The linear displacements along *x, y, z* axes represent the linear motion of the body. Whereas Euler angles (θ_x, θ_y, θ_z) represent the rotational motion of body. For modelling of the body the Newton-Euler equations are used which are for body fixed frame. The body fixed frame is aligned to the inertial frame. The robot body here has six degrees-of-freedom, i.e. three linear motion along *x, y, z* axis and rotational motion demonstrating roll, yaw and pitch. . The body is rotating and translating along the coordinate axis thus demonstrating its motion. This body fixed frame that is aligned with inertial frame is linked to the COG of the body. The *x, y* and *z* axis describes the linear displacements and rotations of body fixed frame. Euler angles demonstrate the orientations of the body. The equations for the forces acting on the body are as follows:

$$\sum F_{\mathrm{x}} = m_{\mathrm{c}}\ddot{x}_{\mathrm{c}} + m_{\mathrm{c}}(\dot{z}_{\mathrm{c}}\dot{\theta}_{\mathrm{cy}} - \dot{y}_{\mathrm{c}}\dot{\theta}_{\mathrm{cz}}) \quad (4.9)$$

$$\sum F_{\mathrm{y}} = m_{\mathrm{c}}\ddot{y}_{\mathrm{c}} + m_{\mathrm{c}}(\dot{x}_{\mathrm{c}}\dot{\theta}_{\mathrm{cz}} - \dot{z}_{\mathrm{c}}\dot{\theta}_{\mathrm{cx}}) \quad (4.10)$$

$$\sum F_{\mathrm{z}} = m_{\mathrm{c}}\ddot{z}_{\mathrm{c}} + m_{\mathrm{c}}(\dot{y}_{\mathrm{c}}\dot{\theta}_{\mathrm{cx}} - \dot{x}_{\mathrm{c}}\dot{\theta}_{\mathrm{cy}}) \quad (4.11)$$

$$\sum M_{\mathrm{x}} = J_{\mathrm{cx}}\ddot{\theta}_{\mathrm{cx}} - \dot{\theta}_{\mathrm{cy}}\dot{\theta}_{\mathrm{cz}}(J_{\mathrm{cy}} - J_{\mathrm{cz}}) \quad (4.12)$$

$$\sum M_{\mathrm{y}} = J_{\mathrm{cy}}\ddot{\theta}_{\mathrm{cy}} - \dot{\theta}_{\mathrm{cz}}\dot{\theta}_{\mathrm{cx}}(J_{\mathrm{cz}} - J_{\mathrm{cx}}) \quad (4.13)$$

$$\sum M_{\mathrm{z}} = J_{\mathrm{cz}}\ddot{\theta}_{\mathrm{cz}} - \dot{\theta}_{\mathrm{cx}}\dot{\theta}_{\mathrm{cy}}(J_{\mathrm{cx}} - J_{\mathrm{cy}}) \quad (4.14)$$

Forces that are developed due to the body fixed frame are represented in Eqs. 4.1–4.3. The gyroscopic moments are represented in Eqs. 4.4–4.6. It is to be observed that the linear velocities and rotation represented in above equations are with reference to body fixed frame. Euler Junction Structure (EJS) demonstrate the Euler equations in bond graph.

Here, a rigid body of mass m is considered, moments of inertia about x, *y* and *z* are represented as *Ixx*, *Iyy* and *Izz*; angular velocities are mentioned as ω_{xx},ω_{xy} and ω_{xz} in reference to body fixed frame when seen from an inertial frame, external moment components are *Mx*, *My* and *Mz*, whereas, external force components are *Fx*, *Fy* and *Fz*. The bond graph of EJS for the body. The gyrator in Newton's equations can be represented in the same form as EJS. All six Newton-Euler equations are represented by combining both the models as shown in Fig. 4.3.

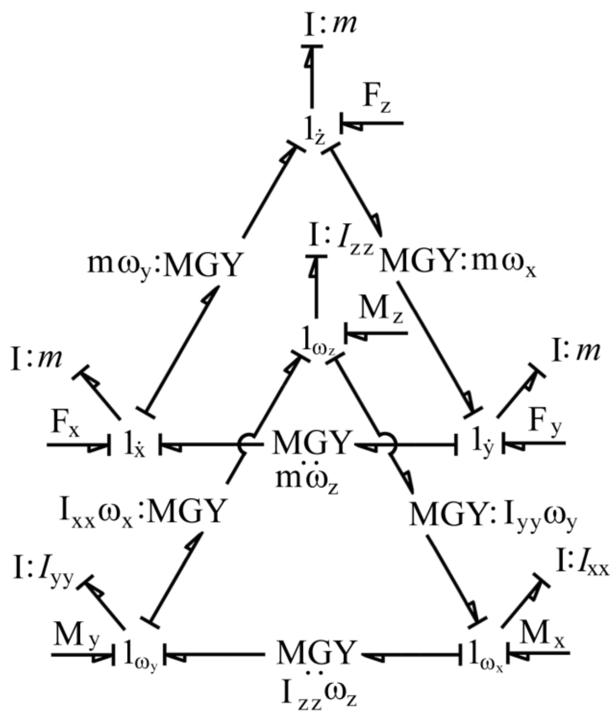

Fig. 4.3 Bond graph of EJS (the bond graph for the body is also same)

Fig. 4.3 is the basis for construction of the bond graph model for the quadruple model. The dynamic constraints are included while implementing the kinematic constrains in the bond graph. The reason for the same is the ruler junction structure which is power conserving in nature. Thus, proving that bond graph modelling is beneficial in systems that are complex in nature. The equation for linear velocities are as follows:

$$\dot{x}_1 = \dot{x}_c + z_1\dot{\theta}_{cy} - y_1\dot{\theta}_{cz} \quad (4.15)$$

$$\dot{y}_1 = \dot{y}_c + x_1\dot{\theta}_{cz} - z_1\dot{\theta}_{cx} \quad (4.16)$$

$$\dot{z}_1 = \dot{z}_c + y_1\dot{\theta}_{cx} - x_1\dot{\theta}_{cy} \quad (4.17)$$

4.3.2 Bond Graph Model

The bond graph of alternative three-dimensional model is represented in Fig. 4.5. The body is modelled as combined EJS for angular as well as linear velocities. The bond graph for body is same as Fig. 4.3. Sub-model for the Link has been represented in Fig. 4.4.

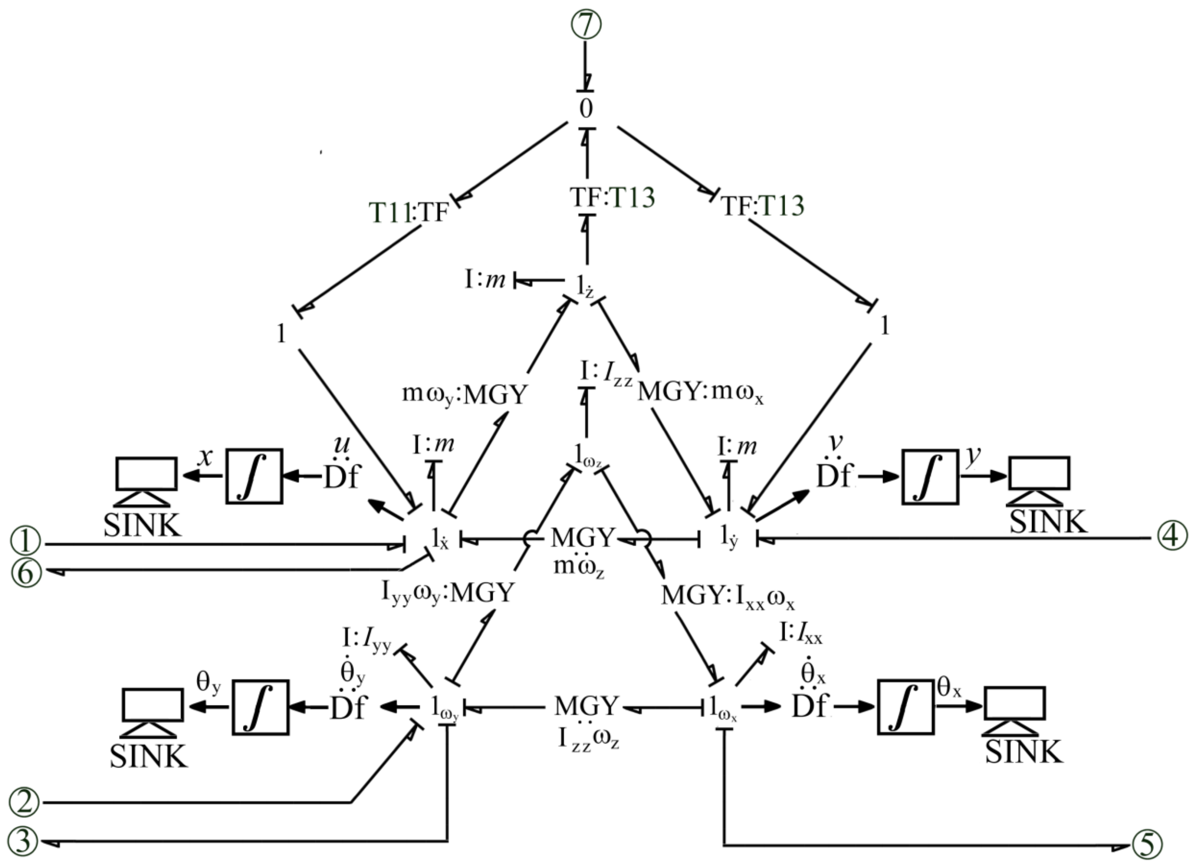

Fig. 4.4 Bond graph model of link

The bond graph for Link1 and Link 2 are same except the port 1. The representations of seven ports are given in Table 4.1. The port 2 causes rotation in y- direction that develops motion in linear x-direction on which the traction force is acting through port 1. Thus, the flow output from Link1 are linked to Link2 and the flow output from Link2 are transferred to the vehicle body. Both the Links are joined by a spring damper system to form leg. The distance of leg from COG of body in x, y and z direction are a, c and h, respectively. The body is connected to the legs through transformers having values a, c and h. As the bond graph of link and body have been already represented in above figures, so, the whole model is represented as a word bond graph in Fig. 4.5.

Table 4.1 Representation of Ports

Port No.	Representation
1	Traction force acting on lower link from ground.
2	Source of effort from motor
3	Flow output from y-direction rotation junction
4	Flow output from y-direction linear junction
5	Flow output from x-direction rotation junction
6	Flow output from x-direction linear junction
7	Weight of link

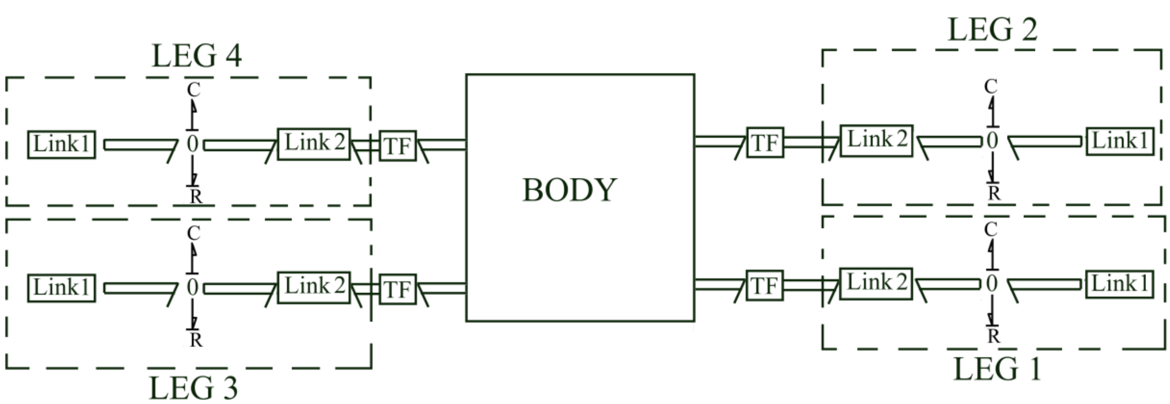

Fig. 4.5 Vector bond graph representation of three-dimensional model

4.4 Parameter Values and Simulation Results

This section discusses the parameters and results for the quadruple model based on planar model and alternative model three-dimensional model. The results presented are for different gaits and robot's stability while undergoing these gaits.

4.4.1 Quadruple moving with Trot Gait

The trot gait is dynamically stable gait and fastest among the gaits discussed in thesis. In the model legs 1-4 and 2-3 are diagonal to each other. Thus, the movement of legs is 1-4 together taking first step and 2-3 moving together during second step. The parameters are shown in Table 4.1.

Table 4.2 Parameter values for trot gait

Parameters	**Description**	**Values**
C_{m}	Capacitance of motor (F)	10
λ	Differentiability constant	7
I_{m}	Moment of inertia of motor (kg m^2)	1
I_{b}	Moment of inertia of body (kg m^2)	10
I_{w}	Moment of inertia of leg (kg m^2)	5
$K_{\mathrm{m_{f1}}}$	Compliance element of front leg's Link1 $(\mathrm{N/m})$	10^8
K_{l}	Compliance element of leg's $(\mathrm{N/m})$	10
$K_{\mathrm{m_{f2}}}$	Compliance element of front leg's Link2 $(\mathrm{N/m})$	10^7
$K_{\mathrm{m_{r1}}}$	Compliance element of rear leg's Link1 $(\mathrm{N/m})$	10^8
$K_{\mathrm{m_{r2}}}$	Compliance element of rear leg's Link2 $(\mathrm{N/m})$	10^6
L_{leg}	Length of complete leg (m)	0.6
l_1, l_2	Distance of front and rear wheel from COG(m)	0.5
M_{b}	Mass of body (kg)	600
R_{m}	Resistance of motor (Ω)	0.1
μ_1	Modulus of Gyrator for motor of front Leg's Link1	2.1
μ_2	Modulus of Gyrator for motor of front Leg's Link2	0.7
μ_3	Modulus of Gyrator for motor of rear Leg's Link1	1.95
μ_4	Modulus of Gyrator for motor of rear Leg's Link2	0.64

The efforts control of leg by mathematical formulations are given to the links. The *x*-direction on positive side shows the forward direction. The time cycle for each step is 1s. The simulation was run for 10s. The result for trot gait are shown in Fig. 4.6.

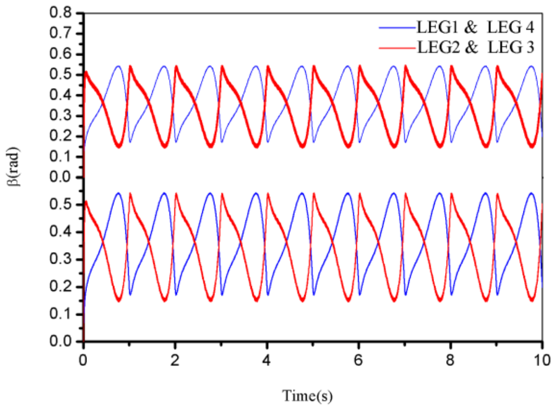

(a)

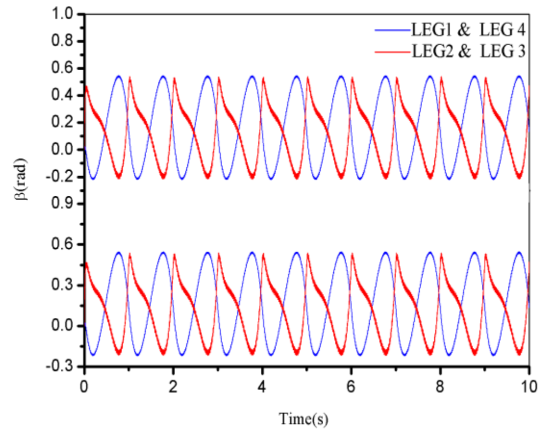

(b)

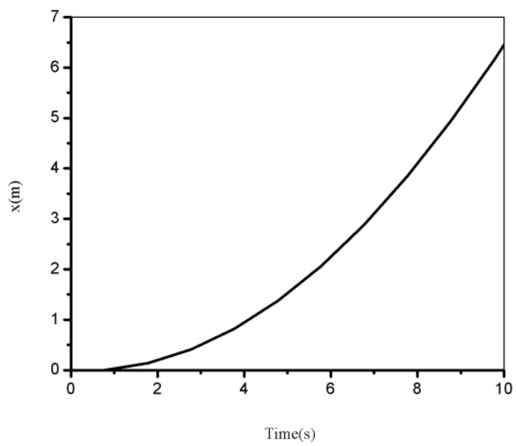

(c)

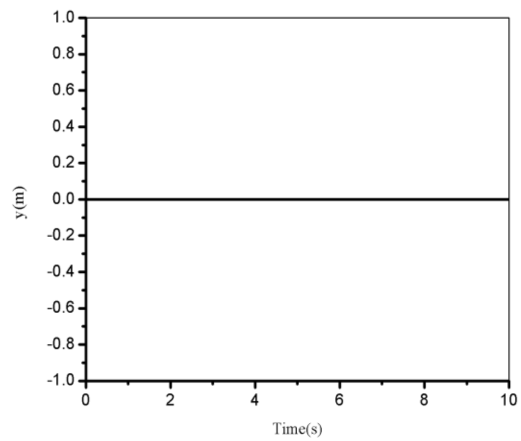

(d)

Fig. 4.6(a) Rotation of Link1, (b) Rotation of Link2, (c)Displacement in *x*-direction and (d) Displacement in *y*-direction

Fig. 4.7(a) and (b) show the rotation of Link1 and Link2 of the all four legs. The graphs clearly show that Leg1-4 and Leg 2-3 are moving together. The displacement in *x*-direction is 6.25 m and there is no displacement in *y*-direction, which depicts that the robot is moving in straight path.

4.4.2 Quadruple moving with Bound Gait

The bound gait is dynamically stable gait and slower than trot gait. In the model Legs 1-3 and 2-4 are on left and right side respectively with respect to body frame. Thus the movement of Legs is 1-3 together taking first step and 2-4 moving together during second step. The parameters are shown in Table 4.2

Table 4.3 Parameter values for bound gait

Parameters	**Description**	**Values**
C_m	Capacitance of motor (F)	10
λ	Differentiability constant	7
I_m	Moment of inertia of motor (kg m^2)	1
I_b	Moment of inertia of body (kg m^2)	10
I_w	Moment of inertia of Leg (kg m^2)	5
$K_{m_{f1}}$	Compliance element of front Leg's Link1 (N/m)	10^8
K_1	Compliance element of leg's (N/m)	10
$K_{m_{f2}}$	Compliance element of front leg's Link2 (N/m)	10^7
$K_{m_{r1}}$	Compliance element of rear leg's Link1 (N/m)	10^8
$K_{m_{r2}}$	Compliance element of rear leg's Link2 (N/m)	10^6
L_{leg}	Length of complete leg (m)	0.6
l_1, l_2	Distance of front and rear wheel from COG (m)	0.5
M_b	Mass of body (kg)	600
R_m	Resistance of motor (Ω)	0.1
μ_1	Modulus of gyrator for motor of front leg's Link1	2.1
μ_2	Modulus of gyrator for motor of front leg's Link2	0.7
μ_3	Modulus of gyrator for motor of rear leg's Link1	1.95
μ_4	Modulus of gyrator for motor of rear leg's Link2	0.64

The efforts control of leg by mathematical formulation are given to the links. The x-direction on positive side shows the forward direction. The time cycle for each step is 1s. The simulation was run for 10s. The result for trot gait are shown in Fig. 4.7.

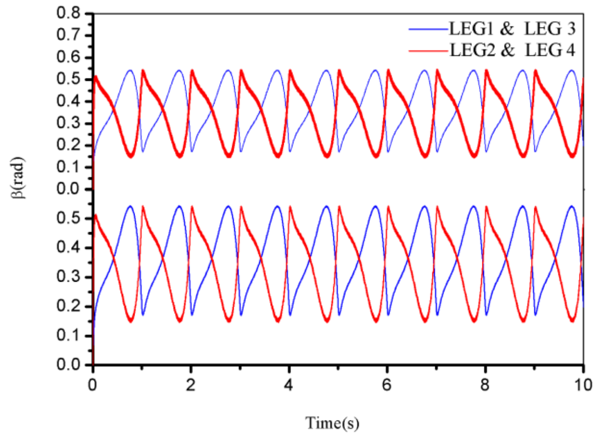

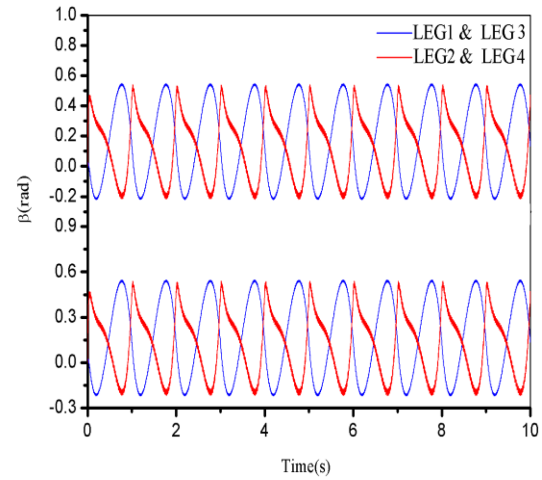

(a) (b)

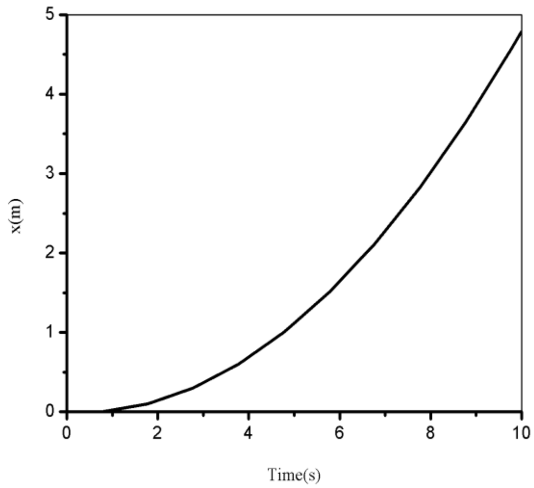

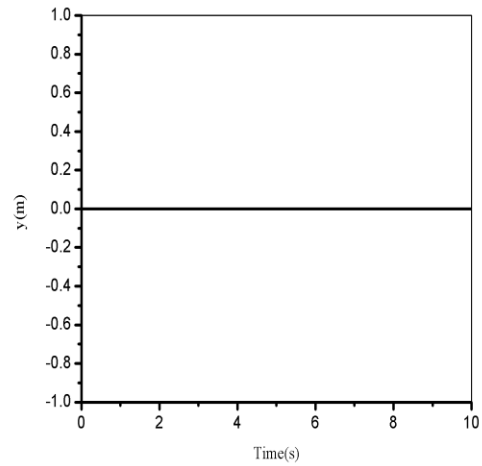

(c) (d)

Fig. 4.7(a) Rotation of link1, (b) Rotation of Link2, (c) Displacement in *x*-direction and (d) Displacement in *y*-direction

Fig. 4.7(a) and (b) show the rotation of Link1 and Link2 of the all four Legs. The graphs clearly show that Leg1-3 and Leg2-4 are moving together. The displacement in *x*-direction is 4.78 m and there is no displacement in *y*-direction, which depicts that the robot is moving in straight path.

4.4.3 Quadruple moving with Pace Gait

The pace gait is dynamically stable gait and speed almost equal to bound gait. In the model Legs 1-2 and 3-4 are front and rear Legs. Thus, the movement of legs is 1-2 are together taking first step and 2-4 are moving together during second step. The parameters are shown in Table 4.3

Table 4.4 Parameter values for pace gait

Parameters	Description	Values
C_{m}	Capacitance of motor (F)	10
λ	Differentiability constant	7
I_{m}	Moment of inertia of motor (kg m^2)	1
I_{b}	Moment of inertia of body (kg m^2)	10
I_{w}	Moment of inertia of leg (kg m^2)	5
$K_{\mathrm{m_{f1}}}$	Compliance element of front leg's Link1 $(\mathrm{N/m})$	10^8
K_1	Compliance element of leg's $(\mathrm{N/m})$	10
$K_{\mathrm{m_{f2}}}$	Compliance element of front leg's Link2 $(\mathrm{N/m})$	10^7
$K_{\mathrm{m_{r1}}}$	Compliance element of rear leg's Link1 $(\mathrm{N/m})$	10^8
$K_{\mathrm{m_{r2}}}$	Compliance element of rear leg's Link2 $(\mathrm{N/m})$	10^6
L_{leg}	Length of complete leg (m)	0.6
l_1, l_2	Distance of front and rear wheel from COG (m)	0.5
M_{b}	Mass of body (kg)	600
R_{m}	Resistance of motor (Ω)	0.1
μ_1	Modulus of gyrator for motor of front leg's Link1	2.1
μ_2	Modulus of gyrator for motor of front leg's Link2	0.7
μ_3	Modulus of gyrator for motor of rear leg's Link1	1.95
μ_4	Modulus of gyrator for motor of rear leg's Link2	0.64

The efforts controlled Leg by mathematical formulation are given to the links. The *x*-direction on positive side shows the forward direction. The time cycle for each step is 1s. The simulation was run for 10s. The result for trot gait are shown in Fig. 4.8.

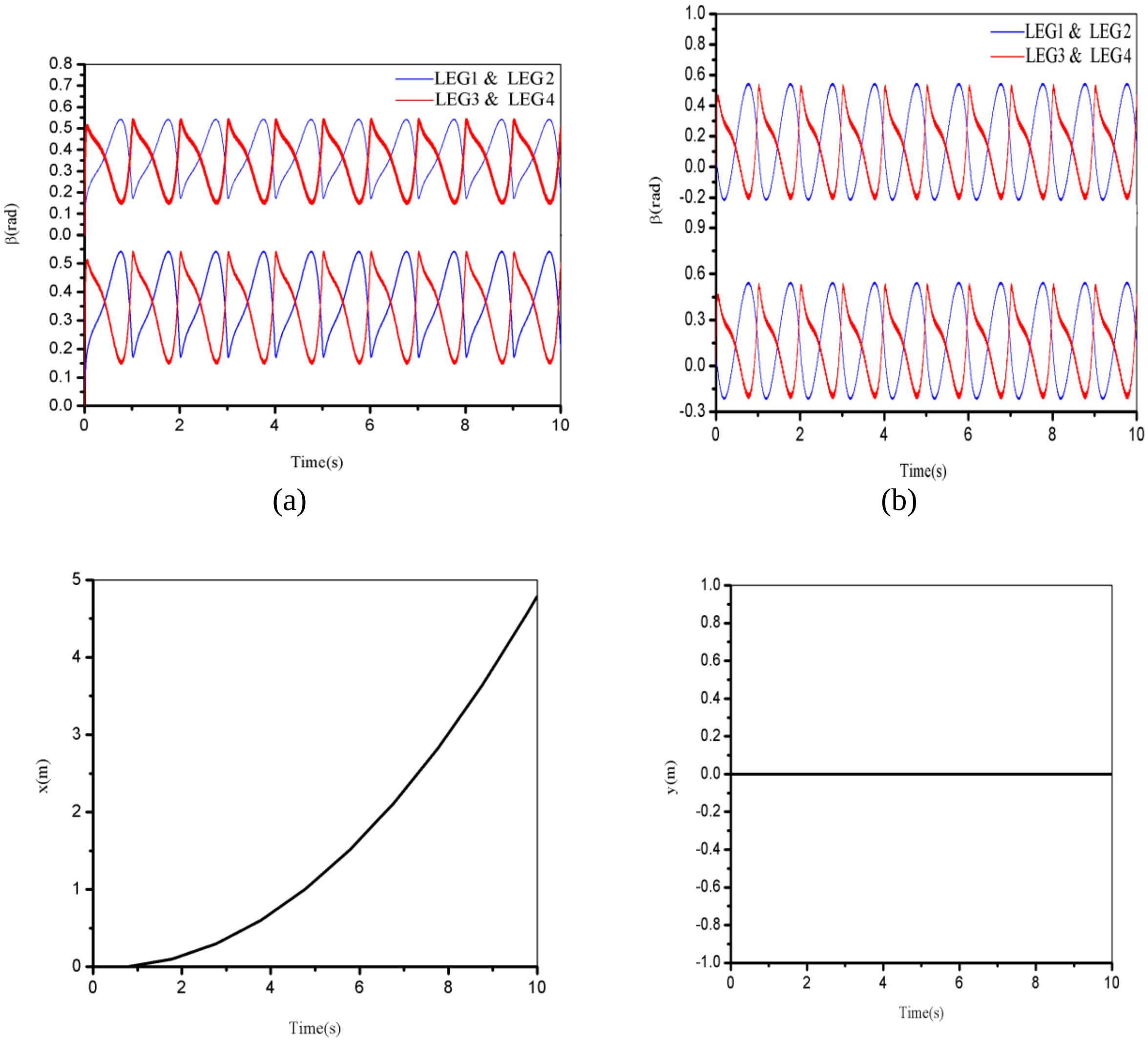

(a) (b)

(c) (d)

.Fig. 4.8(a) Rotation of Link1, (b) Rotation of Link2, (c) Displacement in *x*-direction and (d) Displacement in *y*-direction

Fig. 4.8(a) and (b) show the rotation of Link1 and Link2 of the all four legs. The graphs clearly show that Leg1-2 and Leg3-4 are moving together. The displacement in x-direction is 4.76m and there is no displacement in y-direction, which depicts that the robot is moving in straight path.

4.4.4 Quadruple moving with Amble Gait

The amble gait is statically stable gait and speed is very slow. As explained in Chapter 1 in amble one step moves at a time. As seen in results trot gait is fastest so the same pattern is followed, i.e., 1-4-2-3 is the order of movement of Legs. The parameters are shown in Table 4.4.

Table 4.5 Parameter values for amble gait

Parameters	**Description**	**Values**
C_m	Capacitance of motor (F)	10
λ	Differentiability constant	7
I_m	Moment of inertia of motor (kg m^2)	1
I_b	Moment of inertia of body (kg m^2)	10
I_w	Moment of inertia of leg (kg m^2)	5
$K_{m_{f1}}$	Compliance element of front leg's Link1 (N/m)	10^8
K_l	Compliance element of leg's (N/m)	10
$K_{m_{f2}}$	Compliance element of front leg's Link2 (N/m)	10^7
$K_{m_{r1}}$	Compliance element of rear leg's Link1 (N/m)	10^8
$K_{m_{r2}}$	Compliance element of rear leg's Link2 (N/m)	10^6
L_{leg}	Length of complete leg (m)	0.6
l_1, l_2	Distance of front and rear wheel from COG (m)	0.5
M_b	Mass of body (kg)	600
R_m	Resistance of motor (Ω)	0.1
μ_1	Modulus of gyrator for motor of front leg's Link1	2.1
μ_2	Modulus of gyrator for motor of front leg's Link2	0.7
μ_3	Modulus of gyrator for motor of rear leg's Link1	1.95
μ_4	Modulus of gyrator for motor of rear leg's Link2	0.64

The efforts controlled Leg by mathematical formulation are given to the links. The x-direction on positive side shows the forward direction. The time cycle for each step is 1s. The simulation was run for 10s. The result for trot gait are shown in Fig. 4.9, Fig. 4.10 and Fig. 4.11.

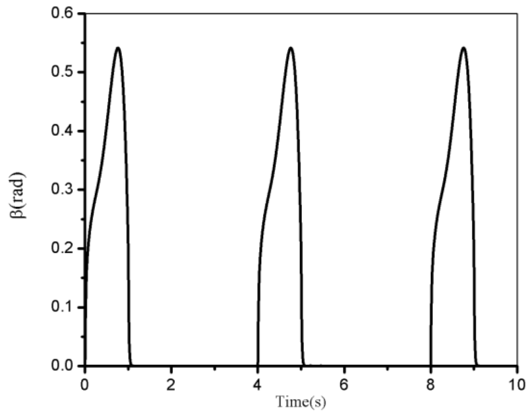

(a)

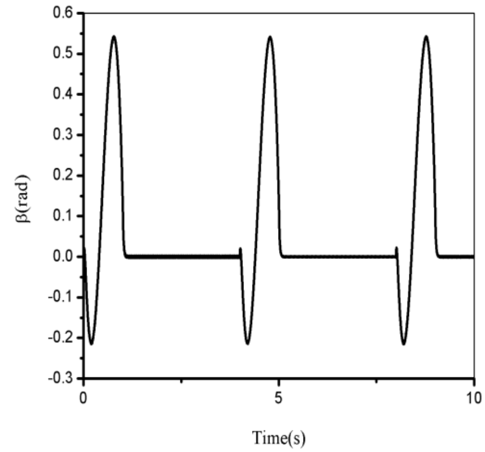

(b)

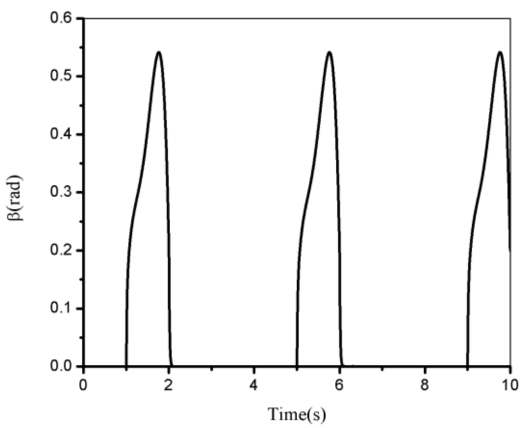

(c)

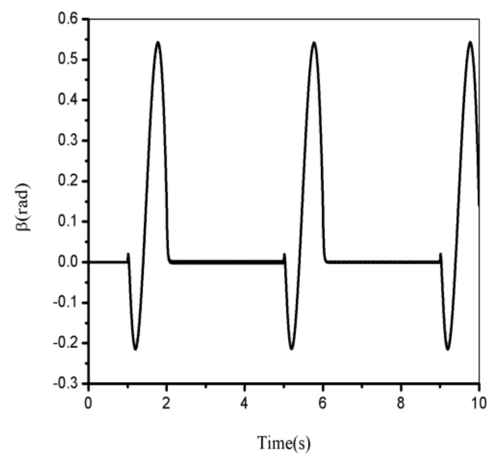

(d)

Fig. 4.9(a) Rotation of Link1 of Leg1, (b) Rotation of Link2 of Leg1, (c) Rotation of Link1 of Leg4 and (d) Rotation of Link2 of Leg4

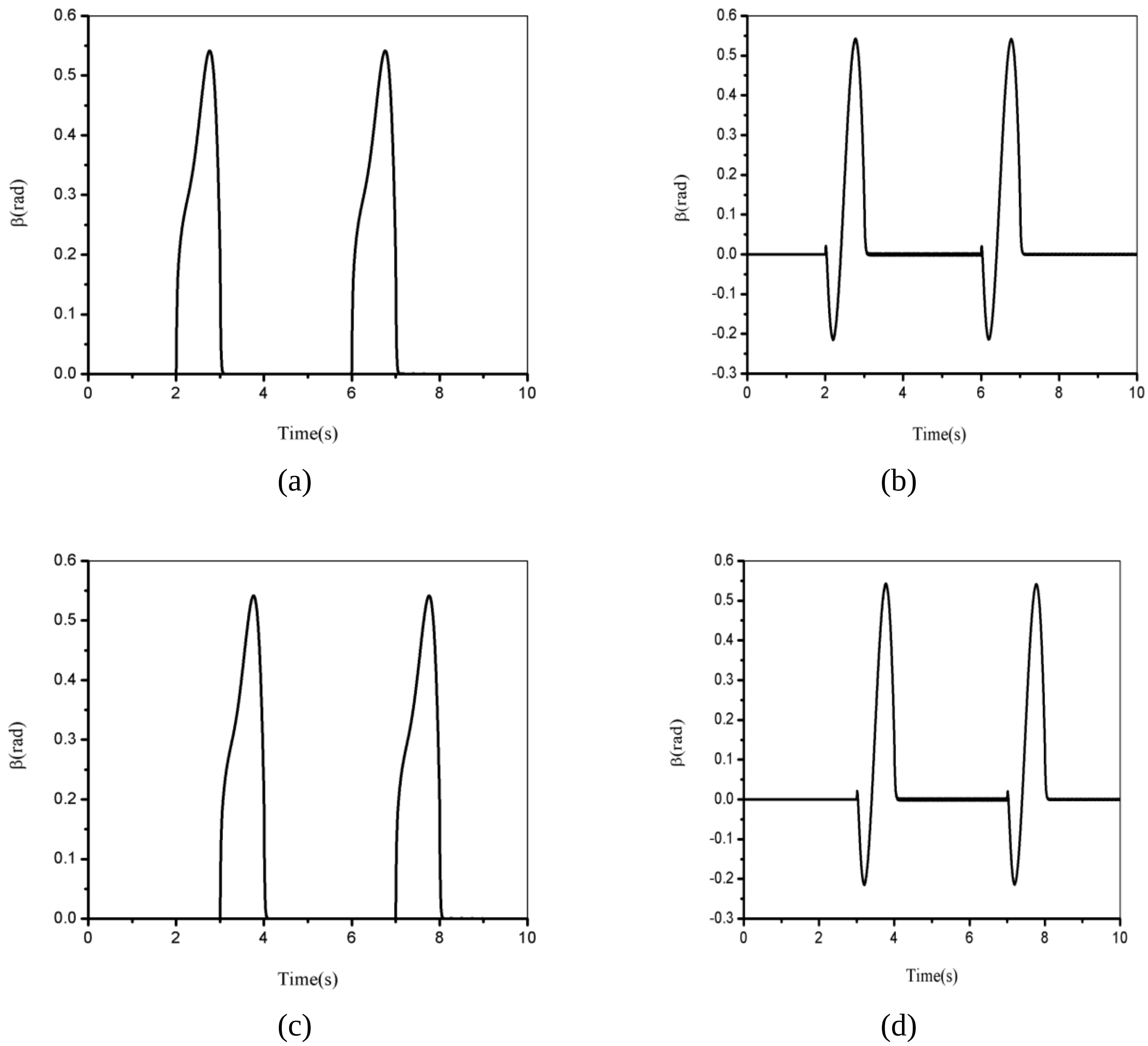

Fig. 4.10(a) Rotation of Link1 of Leg2, (b) Rotation of Link2 of Leg2, (c) Rotation of Link1 of Leg3 and (d) Rotation of Link2 of Leg3

Fig. 4.9 and Fig. 4.10 is shows that Leg1 moves first and then comes down, meanwhile Legs 2,3and4 are on ground giving support to the robot. After 1s, Leg1 touches the ground, Leg4 starts its step, while Leg1, 2and 3 stay on ground. The Leg2 and Leg 3 start at 2s and 3s respectively. The above results clearly show that at every step taken by robot three Legs are on ground. The result for displacement in *x*-direction and *y*-direction are shown in Fig. 4.11.

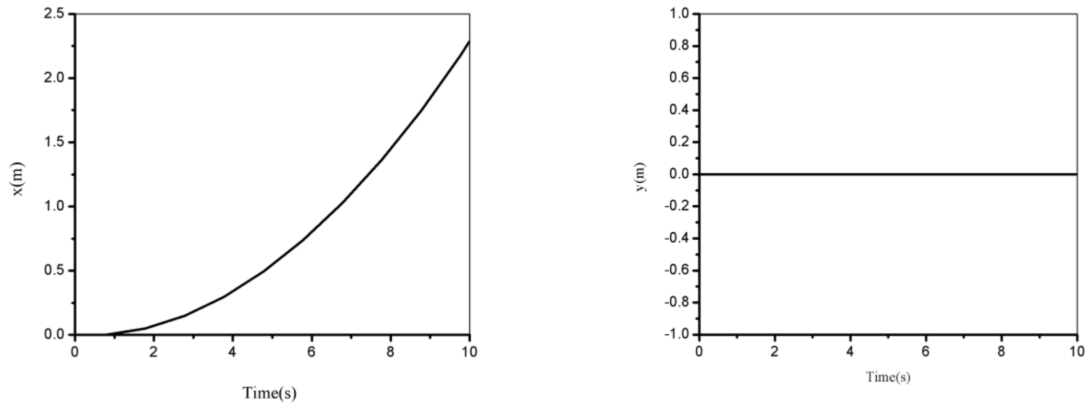

(a) (b)

Fig. 4.11(a) Displacement in *x*-direction and (b) Displacement in *y*-direction

The above result shows that there is displacement of 2.28m in *x*-direction and no displacement in y-direction. Thus, the robot moves in straight path.

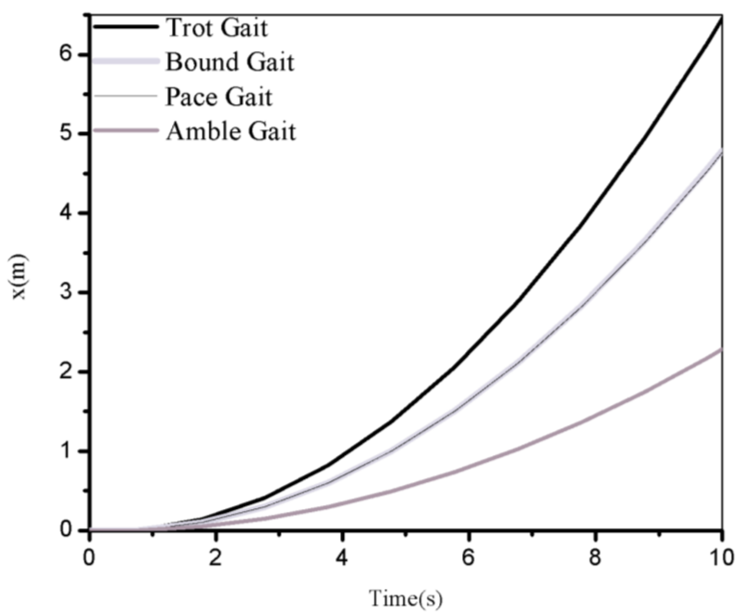

Fig. 4.12 Comparison of displacement of body during four gaits

The Fig.4.12 shows the comparison of displacement achieved during the four gaits. It can be clearly seen that trot is fastest, pace and bound gait are almost equal and amble gait is the slowest. These results completely validate the theory that states that dynamically stable gaits are faster than statically stable gait and also, the trot gait is the fastest.

4.4.5 Alternative Three-Dimensional Model

Pace gait was implemented in this model. The parameters for it are given in Table 4.5.

Table 4.6 Parameter values

Parameters	**Description**	**Values**
C_m	Capacitance of motor (F)	10
λ	Differentiability constant	7
I_{XX}	Moment of inertia of body about x-axis (kg m^2)	10
I_{YY}	Moment of inertia of body about y-axis (kg m^2)	10
I_{ZZ}	Moment of inertia of body about z-axis (kg m^2)	10
$I_{XX_{leg}}$	Moment of inertia of Leg about x-axis (kg m^2)	0.1
$I_{YY_{leg}}$	Moment of inertia of Leg about y-axis (kg m^2)	0.2
$I_{ZZ_{leg}}$	Moment of inertia of leg about z-axis (kg m^2)	0.1
I_m	Moment of inertia of motor (kg m^2)	1
$K_{m_{f1}}$	Compliance element of front leg's Link1 (N/m)	10^8
K_l	Compliance element of leg's (N/m)	10
$K_{m_{f2}}$	Compliance element of front leg's Link2 (N/m)	10^7
$K_{m_{r1}}$	Compliance element of rear leg's Link1 (N/m)	10^8
$K_{m_{r2}}$	Compliance element of rear leg's Link2 (N/m)	10^7
K_{f1}	Compliance element of front leg's suspension (N/m)	10^{10}
K_{r1}	Compliance element of rear leg's suspension (N/m)	10^6
R_f	Damping element of front leg's suspension (Ns/m)	500
R_r	Damping element of rear leg's suspension (Ns/m)	360
L_{leg}	Length of complete leg (m)	0.6
l_1, l_2	Distance of front and rear wheel from COG (m)	0.5
R_m	Resistance of motor (Ω)	0.2
M_b	Mass of body (kg)	540
μ_1	Modulus of gyrator for motor of front leg's Link1	1.95
μ_2	Modulus of gyrator for motor of front leg's Link2	0.64
μ_3	Modulus of gyrator for motor of rear leg's Link1	2.1
μ_4	Modulus of gyrator for motor of rear leg's Link2	0.7

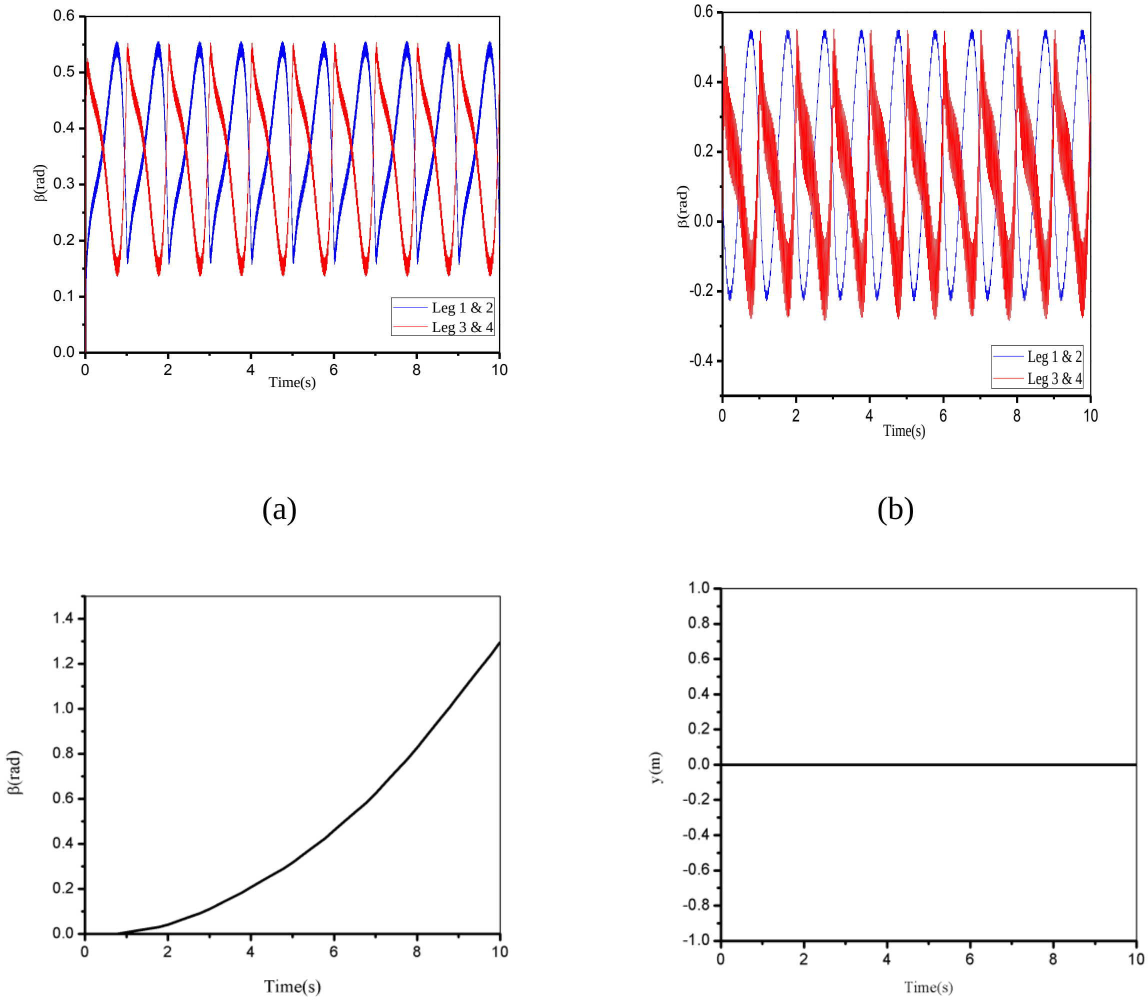

(a) (b)

(c) (d)

Fig. 4.13(a) Angular motion of Link1, (b) Angular motion of Link1, (c) Displacement in x-axis and (d) Displacement in y direction

The efforts controlled leg by mathematical formulation are given to the links. The *x*-direction on positive side shows the forward direction. The time cycle for each step is 1s. The simulation was run for 10s. The maximum angular rotation is 0.55 rad and the displacement in *x*-direction is 1.3m.

Chapter 5

Conclusions

1.3 Conclusions

The main emphasis of the thesis was to achieve the stability for dynamically and statically balanced gaits. In addition, the implementation of these gaits was of main concern. The bond graphs for the two legged and quadruple robot were developed. Two models were developed for quadruple model, where planar model had both dynamically and statically stable gaits. For three-dimensional model, dynamically stable gaits were implemented only. The following conclusions can be drawn from the thesis.

- The simulations of the models developed in this work present good quality results. The results for the models are very much similar to the gaits followed by animals in real life and also in harmony with work done by others. The first model discussed in this thesis focused on two-legged robot, the results for the link's modeled for it were found accurate for quadruple robot also. The data generated by Matlab for mathematical formulation gave accurate results in bond graph. So, this shows the reliability of bond graph as a tool in field of modelling techniques.

- A detailed observation of the graphs obtained gives us very minute details about the movement of legs. For example: As leg takes step forward the lower Link2 goes backward and upper Link1 moves forward, whereas both the links reach their peak amplitude together and come down at the same time.

- Another observation depicts a phase lag in the movement of links of legs taking the steps simultaneously. This phase lag is because when the leg taking first step will come down the leg taking next step will start lifting up to maintain continuous movement.

- The next models which are a quadruple robot modelled as planar and three dimensional model focused on implementing of gaits. The results generated prove the stability of model for both dynamically and statically stable gaits. Observing the results, it is seen that present model is stable irrespective of the gaits being followed and moves forward.

- As noticeable from the comparison of the displacement achieved by the gaits implemented, it is observed that the dynamically balanced gaits are faster and more energy efficient then statically stable gaits as they traverse more distance then statically balanced gaits.

- Another observation is that the trot gait is the most energy efficient as it traverses the maximum distance among all the gaits.

- A quick look at comparison between at distance travelled by the same gait in three-dimensional model shows that it is more than planar quadruple model. Thus, three-dimensional model proves to be more energy efficient than planar quadruple model.

1.4 Future Scope

Based on the work presented in this thesis, the following work is suggested for future:

- The models developed here walk only in straight path and thus, further work is to develop model that can turn.

- Since the model could not turn and so, it was not possible to add some control on it like trajectory tracking. Thus, work can be done to add some modern control techniques for making the model more independent.

- Another plan for future is to develop a physical model for the models discussed here to realize how it will work in actuality. Also, it was not possible to implement all the gaits in three dimensional model which is more efficient, so, immediate target would be to do the same.

References

[**1**] F. Iida, G. Gomez, R. Pfeifer, "Exploiting body dynamics for controlling a running quadrupe robot," *2005 Int. Conf. Adv. Robot. ICAR '05, Proc.*, vol. 2005, pp. 229–235, 2005.

[**2**] M. Raibert, "BigDog, the rough-terrain quadruped robot," *IFAC Proc. Vol.*, vol. 17, no. 1 PART 1, pp. 6–9, 2008.

[**3**] X. Rong, Y. Li, J. Ruan, B. Li, "Design and simulation for a hydraulic actuated quadruped robot," *J. Mech. Sci. Technol.*, vol. 26, no. 4, pp. 1171–1177, 2012.

[**4**] C. Semini, N. G. Tsagarakis, E. Guglielmino, M. Focchi, F. Cannella, D. G. Caldwell, "Design of HyQ – a hydraulically and electrically actuated quadruped robot," *Proc. Inst. Mech. Eng. Part I J. Syst. Control Eng.*, vol. 225, no. 6, pp. 831–849, 2011.

[**5**] C. D. Remy, R. Siegwart, C. Gehring, M. Bloesch, M. a. Hoepflinger, M. Hutter, "A Compliant Quadrupedal Robot for Fast, Efficient, and Versatile Locomotion," *15th Int. Conf. Climbing Walk. Robot - CLAWAR 2012*, pp. 1–8, 2012.

[**6**] A. Nagakubo, S. Hirose, "Walking and Running of the Quadruped Wall-Climbing Robot," *Proc. 1994 IEEE Int. Conf. Robot. Autom.*, vol. 2, pp. 1005–1012, 2002.

[**7**] E. Gilbert, D. Johnson, "Distance functions and their application to robot path planning in the presence of obstacles," *IEEE J. Robot. Autom.*, vol. 1, no. 1, pp. 21–30, 1985.

[**8**] M. H. Raibert, "Trotting , Pacing and Bounding By a Quadruped Robot,"*Journal of Biomechanics*, vol. 23, no. 1, pp.79-98,1990.

[**9**] C. D. Remy *et al.*, "Walking and crawling with ALoF: a robot for autonomous locomotion on four legs," *Ind. Robot An Int. J.*, vol. 38, no. 3, pp. 264–268, 2011.

[**10**] M. Hardt, O. Von Stryk, "Towards Optimal Hybrid Control Solutions for Gait Patterns of a Quadruped," *3rd Int. Conf. Climbing Walk. Robot.*, vol. 2000, pp. 385–392, 2000.

[**11**] J. Y. Kim, I. W. Park, J. H. Oh, "Walking control algorithm of biped humanoid robot on uneven and inclined floor," *J. Intell. Robot. Syst. Theory Appl.*, vol. 48, no. 4, pp. 457–484, 2007.

[**12**] BJ. Zico Kolter, Mike P. Rodgers, "A Control Architecture for Quadruped Locomotion Over Rough Terrain," *J. Sound Vib.*, vol. 1, no. 1, pp. 1–8, 2013.

[**13**] A. Shkolnik, M. Levashov, I. R. Manchester, R. Tedrake, "Bounding on rough terrain with the LittleDog robot," *Int. J. Rob. Res.*, vol. 30, no. 2, pp. 192–215, 2011.

[**14**] P. Krishna, "Dynamic Gaits and Control in Flexible Body Quadruped Robot," *Proc. 1st 16th ...*, pp. 706–713, 2013.

[**15**] H. Kimura, I. Shimoyama, H. Miura, “Dynamics in the dynamic walk of a quadruped robot,” *Adv. Robot.*, vol. 4, no. 3, pp. 283–301, 1989.

[**16**] M. Migdalovici, L. Vlədəreanu, D. Baran, G. Vlədeanu, M. Radulescu, “Stability Analysis of the Walking Robots Motion,” *Procedia Comput. Sci.*, vol. 65, no. Iccmit, pp. 233–240, 2015.

[**17**] T. K. Bera, K. Bhattacharya, A. K. Samantaray, “Evaluation of antilock braking system with an integrated model of full vehicle system dynamics,” *Simul. Model. Pract. Theory*, vol. 19, no. 10, pp. 2131–2150, 2011.

[**18**] C. Gehring, S. Coros, M. Hutter, M. Bloesch, M. A. Hoepflinger, R. Siegwart, “Control of dynamic gaits for a quadrupedal robot,” *Proc. - IEEE Int. Conf. Robot. Autom.*, pp. 3287–3292, 2013.

[**19**] M. M. Gor, P. M. Pathak, A. K. Samantaray, J. M. Yang, S. W. Kwak, “Control oriented model-based simulation and experimental studies on a compliant legged quadruped robot,” *Rob. Auton. Syst.*, vol. 72, pp. 217–234, 2015.

[**20**] V. L. Krishnan, P. M. Pathak, S. C. Jain, A. K. Samantaray, “Reconfiguration of four-legged walking robot for actuator faults,” *Proc. Inst. Mech. Eng. Part I J. Syst. Control Eng.*, vol. 226, no. 1, pp. 11–26, 2011.

[**21**] G. Kumar K, P. M. Pathak, “Dynamic modelling & simulation of a four legged jumping robot with compliant legs,” *Rob. Auton. Syst.*, vol. 61, no. 3, pp. 221–228, 2013.

[**22**] M. L. M. Peisun, “A STUDY OF TURNING GAIT CONTROL FOR QUADRUPED WALKING VEHICLE,” pp. 9–12, 1991.

[**23**] M. Fujita and H. Kitano, “Development of an Autonomous Quadruped Robot for Robot Entertainment,” *Auton. Robots*, vol. 5, pp. 7–20, 1998.

[**24**] M. G. Chun, “An Optimal Turning Gait for,” *Intelligence for Mechanical Systems, Proceedings IROS*, no. 91, 1991.

[**25**] A. Shkolnik, M. Levashov, I. R. Manchester, and R. Tedrake, “Bounding on rough terrain with the LittleDog robot,” *Int. J. Rob. Res.*, vol. 30, no. 2, pp. 192–215, 2011.